Green Energy and Intelligent Transportation 4 (2025) 100283

Contents lists available at ScienceDirect

Green Energy and Intelligent Transportation

journal homepage: www.journals.elsevier.com/green-energy-and-intelligent-transportation

Full length article

Multi-objective charging scheduling for electric vehicles at charging stations with renewable energy generation

Lei Zhang [a,b,*], Yingjun Ji [a,b], Xiaohui Li [a,b], Zhijia Huang [a,b], Dingsong Cui [c], Haibo Chen [c], Jingyu Gong [d], Fabian Breer [d], Mark Junker [d], Dirk Uwe Sauer [d]

[a] Collaborative Innovation Center for Electric Vehicles in Beijing, Beijing Institute of Technology, Beijing 100081, China
[b] National Engineering Research Center for Electric Vehicles, Beijing Institute of Technology, Beijing 100081, China
[c] Institute for Transport Studies, University of Leeds, 34-40 University Road, Leeds LS2 9JT, UK
[d] Institute for Power Electronics and Electrical Drives, RWTH Aachen University, 52056 Aachen, Germany

HIGHLIGHTS

- A charging behaviour database is built using massive EV operating data.
- A charging scheduling scheme is proposed for a public charging station.
- A charging pile allocation method is presented for charging power control.
- A micro-grid system model is developed for renewable energy integration.
- Simulation studies verify the effectiveness of the proposed scheme.

GRAPHICAL ABSTRACT

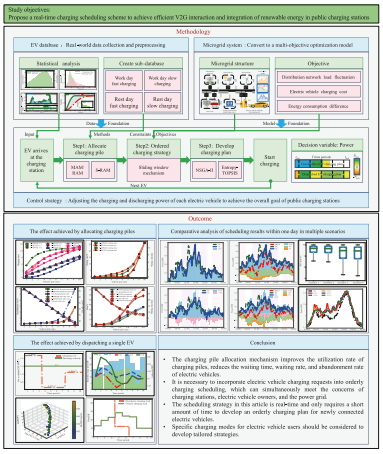

ARTICLE INFO

Keywords:
Electric vehicles
Charging stations
Micro-grid
V2G
Charging scheduling

ABSTRACT

The rapid adoption of electric vehicles (EVs) in recent years has posed significant challenges to the safe operation of local grids, particularly due to massive charging operations at public charging stations. This paper proposes a real-time charging scheduling scheme to enable efficient Vehicle-to-Grid (V2G) interactions and facilitate renewable energy integration at public charging stations while accounting for real-world EV charging behaviors. First, an EV charging/discharging behavior database is developed to capture the temporal uncertainty and charging characteristics of both fast- and slow-charging operations on weekdays and weekends. Then a charging pile allocation mechanism is introduced to optimize the charging power distribution for each EV to maximize the operational efficiency of the studied charging station. A micro-grid system model is developed by incorporating efficient V2G interactions and renewable energy integration. Finally, a comprehensive charging scheduling scheme is proposed to achieve a balanced optimization of multiple objectives. Extensive simulation studies are

* Corresponding author. Collaborative Innovation Center for Electric Vehicles in Beijing, Beijing Institute of Technology, Beijing 100081, China.
E-mail address: lei_zhang@bit.edu.cn (L. Zhang).

https://doi.org/10.1016/j.geits.2025.100283
Received 19 December 2024; Accepted 19 February 2025
Available online 1 March 2025

conducted to evaluate the performance of the proposed scheduling method. The results demonstrate that the proposed scheme achieves strong performance across all three selected indicators.

1. Introduction

1.1. Background

Electric vehicles (EVs) have been widely recognized as a viable solution to address the challenges of global warming and fossil fuel depletion [1–3]. Their synergistic development with renewable energy generation is expected to accelerate the achievement of carbon neutrality [4,5]. In recent years, with continuous technological advancements and supportive government policies, the adoption of EVs has been accelerating rapidly worldwide [6]. To meet the growing charging demands, charging infrastructure, especially public charging stations, is being extensively deployed [7]. However, uncontrolled large-scale charging operations pose significant challenges to the safe operation of the electricity grid [8]. Although grid reinforcements could be a solution, their feasibility is constrained by exorbitant costs [9]. On the other hand, the connection time at a charging station significantly exceeds the time required to meet the charging demand for most EV charging sessions [10]. This provides great opportunities for implementing efficient charging scheduling strategies. By reasonably arranging the charging time, it is possible to reduce the risk of grid overload, lower the charging costs for users, and promote the integration of renewable energy generation [11].

1.2. Literature review

Although uncoordinated charging of EVs may have detrimental effects on the electricity grid [12,13], EVs can also function as flexible energy storage devices to support grid operation through Vehicle-to-Grid (V2G) interactions [14]. Especially in micro-grid systems, EVs can be integrated as distributed energy resources, which is conducive to better adapting to the intermittent characteristics of renewable energy generation [15,16]. Efficient charging scheduling holds the key to realizing these potentials.

Analyzing EV charging behaviors is of great significance for formulating effective charging scheduling schemes [17,18]. In existing research, time [19], spatial [20], or energy models [21] are often used to characterize the charging behaviors of EVs. When modeling the charging behaviors of EVs at public charging stations, statistical fitting is a commonly used method [22]. Generally, it involves constructing time and energy models based on comprehensive charging behavior data [23]. However, this approach has limitations in capturing EV charging behaviors in specific scenarios and fails to fully reflect the inherent heterogeneity of EV charging patterns.

Substantial efforts have also been made to develop efficient charging scheduling schemes [24,25]. From the perspective of control architecture, existing methods can be categorized into centralized control [26], distributed control [27] and hierarchical control [28]. The centralized control method directly regulates EV charging operations at the involved charging stations. Although it is straightforward to implement, it requires a high control frequency. The distributed control method typically uses Time-of-Use (TOU) pricing to encourage EVs to participate in smart charging schemes, but its effectiveness highly depends on the responsiveness of EV users. The hierarchical control method combines the characteristics of centralized and distributed control approaches. It formulates multiple optimization objectives from the perspectives of different stakeholders [29], such as grid operation, financial benefits, and environmental considerations. For grid operation, the optimization objectives may include preventing grid overload, minimizing peak-load differences, reducing distribution losses, and facilitating frequency regulation [30,31]. Financial benefits usually focus on the interests of the power grid, charging stations, and EV users. Environmental considerations may involve carbon emissions reduction and renewable energy integration [32]. Weighting the multi-objective function is a common optimization method for solving such problems [33]. Key control variables include charging time [34], charging/discharging tariffs [35], and charging/discharging power [36,37].

At public charging stations, a micro-grid is often implemented to better accommodate renewable energy generation. Many studies have been conducted on this topic as shown in Table 1. Some key considerations include EV model diversity, uncertainty in renewable energy generation, impact of TOU pricing, and real-time scheduling (RTS). However, existing studies usually address only one or several of these aspects, and there is a lack of research that simultaneously considers all of them. Meanwhile, when formulating specific charging schedules, it is often assumed that sufficient charging piles are available. Nevertheless, this assumption may not conform to the actual situation. Especially during peak charging periods, public charging stations are often fully occupied by EVs, and newly arriving vehicles may have to wait or leave without fulfilling their charging needs at a particular charging station [38,39]. In addition, previous research on EV charging scheduling mainly focuses on single-objective optimization or transforms multiple objectives into a single objective through weighted formulations [40]. These methods rely on static scheduling schemes, which lack flexibility and adaptability to dynamic changes in the actual charging process, such as fluctuations in renewable energy generation, changes in EV arrival times, and variations in grid conditions. Moreover, most of the existing studies assume idealized EV charging demands and behaviors, lacking support

Table 1
Comparison with similar works published in recent years. (MO: Multi-Objective, MS: Multi-Scenario, MM: Multi-charging Modes, MP: Multi-power Pile, DV: Decision Variable, PV: Photovoltaic, WT: Wind Turbine, DN: Distribution Network, G2V: Grid-to-Vehicle.)

Refs.	MO	MS	MM	MP	DV	EV	PV	WT	Load	DN	G2V	V2G	TOU	RTS
[20]	✓	✓	×	×	Price	✓	✓	✓	✓	✓	✓	✓	✓	✓
[34]	✓	✓	✓	×	Time	✓	×	×	×	×	✓	×	×	×
[35]	✓	✓	×	×	Price	✓	✓	×	✓	✓	✓	✓	✓	✓
[36]	×	✓	×	×	Power	✓	×	✓	×	×	✓	✓	×	✓
[37]	×	✓	×	×	Power	✓	✓	×	✓	×	✓	×	✓	×
[41]	✓	✓	×	×	Power	✓	✓	✓	×	×	✓	✓	✓	✓
[42]	✓	✓	×	×	Price	✓	✓	✓	✓	✓	✓	✓	✓	✓
[43]	✓	✓	×	×	Time	✓	×	×	×	×	✓	×	×	✓
[44]	✓	✓	×	×	Price	✓	×	×	×	×	✓	✓	✓	✓
[45]	✓	✓	×	×	Price	✓	×	✓	✓	✓	✓	✓	✓	✓
[46]	✓	✓	×	×	Price	✓	✓	×	✓	✓	✓	✓	✓	✓
[47]	✓	✓	×	×	Price	✓	✓	✓	×	✓	✓	✓	✓	✓
This work	✓	✓	✓	✓	Power	✓	✓	✓	✓	✓	✓	✓	✓	✓

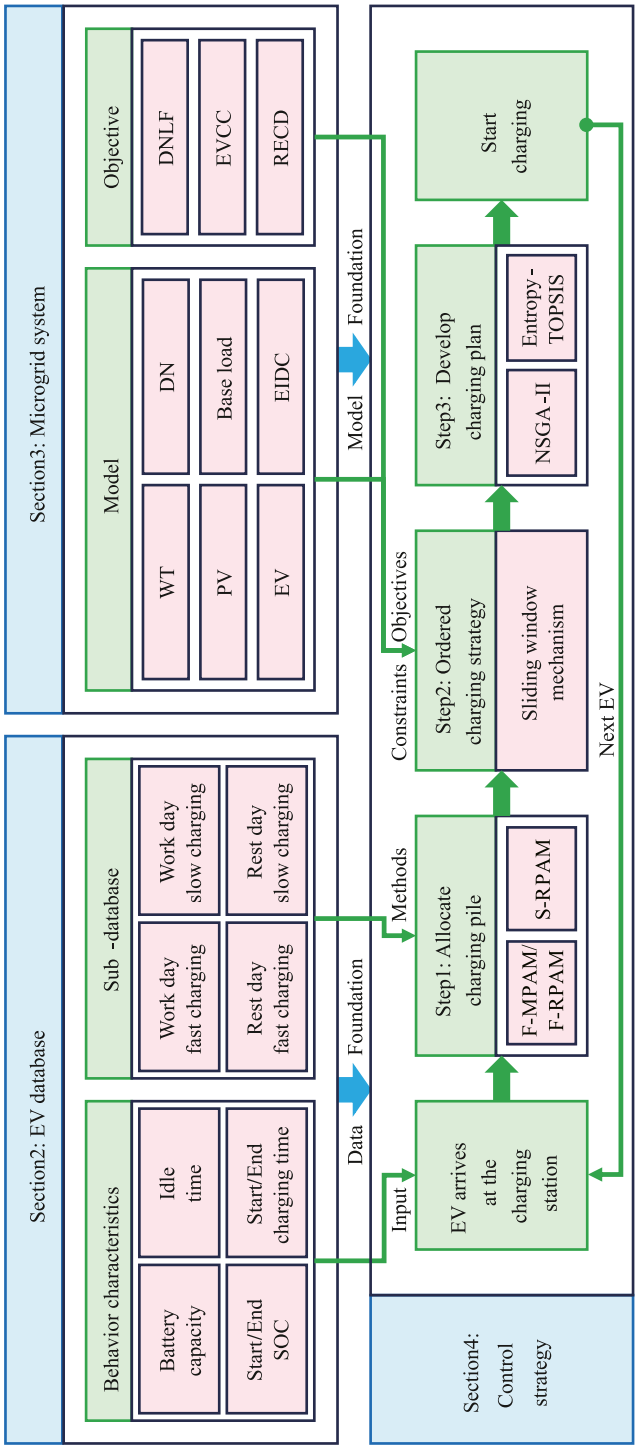

Fig. 1. Schematic of the proposed charging scheduling scheme for electric vehicles at public charging stations.

Table 2
Nomenclature.

$Price_{cha}$/(CNY·kWh^{-1})	Charging electricity price
$Price_{dis}$/(CNY·kWh^{-1})	Discharging electricity price
F–C	Fast charging
S–C	Slow charging
BL	Base load
OTL	Total load of orderly charging
DTL	Total load of disorderly charging
D-C	Disorderly charging
O–C	Orderly charging
SE	SOC_{error}
DL	Disorderly charging EV load
OL	Orderly charging EV load
EVN	Total number of EVs
POCN	Number of EVs participating in orderly charging
ACN	Number of EVs abandoned for charging
WCN	Number of EVs waiting to be charged
FSN	Number of failed solutions
AST/s	Average solving time

from real-world data, which may lead to deviations between the proposed scheduling strategies and actual operation scenarios.

1.3. Contributions

In summary, existing studies have certain limitations in terms of data support, objective consideration, and scheduling flexibility. To address these issues, this study proposes a real-time charging scheduling scheme to facilitate efficient renewable energy integration and V2G interactions at a public charging station with a micro-grid system. First, an EV charging behavior model based on real-world charging data is developed. The dataset consists of 329,632 charging samples collected from 1268 charging stations in Beijing, covering the period from January 1, 2023, to February 19, 2023. Then a multi-objective charging scheduling model is formulated with renewable energy integration, along with a charging pile allocation mechanism and an optimization scheduling method. The Pareto front solution set is derived using the Non-dominated Sorting Genetic Algorithm II (NSGA-II) [48], and the optimal solution is determined using the Entropy and Technique for Order Preference by Similarity to an Ideal Solution (Entropy-TOPSIS) [49]. The main contributions of this study are summarized as follows:

1. A charging scheduling model based on real-world data and a multi-objective optimization framework is adopted. It can provide charging scheduling strategies for different scenarios.
2. A charging pile allocation mechanism is designed to address the limited availability of charging piles. It aims to maximize charging pile utilization while minimizing waiting times and charging abandonment rate.
3. An efficient charging scheduling model is proposed, taking into account grid operation, financial benefits, and renewable energy integration. It can effectively balance the conflicting objectives among different stakeholders.
4. A sliding window mechanism is developed to connect the microscopic EV charging behaviors with the macroscopic operational objectives of the charging station. It enables real-time adjustment of charging schedules according to the actual situation, thereby improving the adaptability of the scheduling scheme.

The remainder of the paper is organized as follows. Section 2 introduces the constructed EV charging behavior dataset and details the extraction of EV charging behavior characteristics. Section 3 presents the multi-objective optimization model for a charging station with renewable energy integration. Section 4 elaborates on the charging pile allocation mechanism and the charging scheduling model formulation. Section 5 provides case studies under typical operating conditions, with

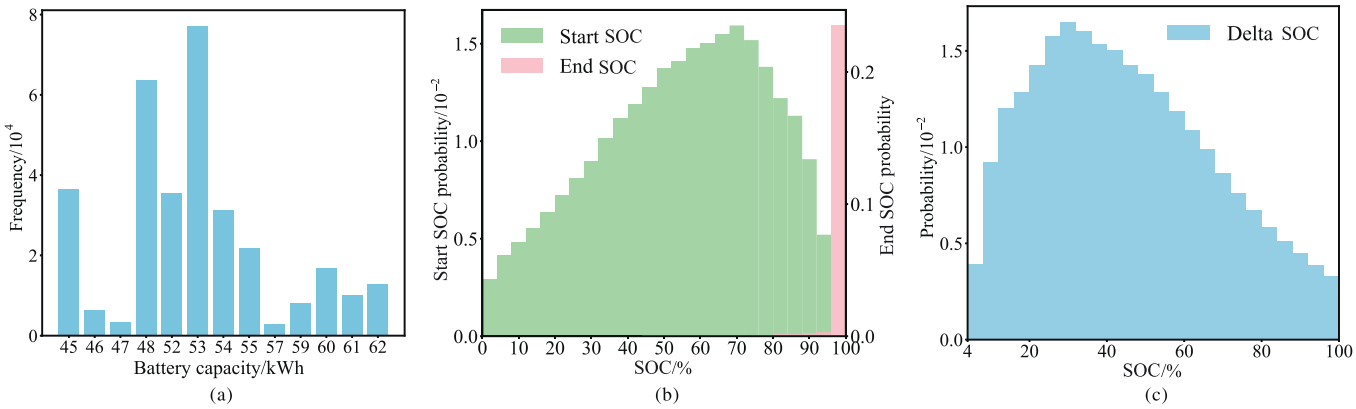

Fig. 2. EV charging characteristics distributions: (a) Battery capacity. (b) Starting and ending SOC. (c) SOC variation.

key conclusions summarized in Section 6. The schematic of the proposed charging scheduling scheme is illustrated in Fig. 1.

2. Analysis of EV charging behaviors

In this section, an EV charging behavior database is developed using real-world charging data collected from 46 charging stations in Beijing. The raw data contains some anomalies, redundancies, and missing values. After data processing, relevant information from some entries in the database is listed in Appendix Table A-2. Each data sample includes battery capacity, starting SOC, ending SOC, and start and end charging times. Based on weekdays and holidays, as well as fast and slow charging, the charging behaviors of different EVs were categorized into four sub-databases, from which charging behavior characteristics are extracted.

2.1. Battery capacity and SOC distribution

The battery capacities of EVs are distributed mainly between 45 kWh and 62 kWh, as depicted in Fig. 2(a). Fig. 2(b) and (c) illustrate the starting SOC, ending SOC, and SOC variation. It can be observed that EVs tend to recharge even when their remaining SOCs are relatively high, and the vast majority of them have an ending SOC of 100%. The SOC variation during a single charging session predominantly falls within the range of 20%–60%.

2.2. Arrival time

In this study, 4:00 am is designated as the start of a day with the lowest probability of EV arrival, and the day ends at 4:00 am the next day. The day is divided into 96 time intervals, each with a duration of 15 mins. When charging piles are available, the arrival time at the charging station is considered as the start charging time. The distribution of EV arrival times is shown in Fig. 3.

As can be seen from Fig. 3, there is no significant peak in the arrival time of fast-charging EVs. On weekdays, the arrival time of slow-charging EVs exhibits two peaks, one in the morning and the other in the evening; on weekends, there is only one peak in the evening. The statistical results reveal the randomness of EV arrival times at the charging station and the differences in EV charging behaviors between weekdays and weekends. To mitigate the influence of outliers, the Gaussian Mixture Model (GMM) is employed for curve fitting, and a residual analysis is also conducted [50,51]. It can be seen that the residual between the fitted curve and the original data fluctuates around 0, indicating that the fitted curve provides a good approximation. Normalizing the values obtained from the GMM fitting yields the probability distribution of EV arrivals within one day. In the simulation, EV information is extracted from the constructed EV behavior database.

2.3. EV charging and parking durations

EVs usually start charging immediately upon arrival at the charging station and continue to park for some time after charging completion. The duration of parking after charging operation is defined as the idle time. The distributions of EV charging and parking durations are presented in Fig. 4.

It can be noted that most fast-charging EVs can reach their target SOCs within 3 h and stay for over 1 h after charging completion. Most slow-charging EVs can reach their target SOCs within 8 h and stay for over 10 h after charging completion. The idle time after EV charging completion provides an opportunity for charging scheduling. By making use of this idle time, the overall EV charging load can to some extent be shifted, thereby reducing the impact of EV charging on the grid.

3. Optimization model

The studied charging station is integrated into a micro-grid with renewable energy generation, as shown in Fig. 5. An Energy Information Dispatch Center (EIDC) is responsible for regulating the power flows among different units, and the distribution network serves as an auxiliary power source. When the power supply exceeds the power demand, the excess energy is either consumed by the basic power usage of the charging station or transferred to other nodes in the distribution network. As depicted in Fig. 6, the EV charging/discharging process is divided into T time slots, each with an interval of Δt. The power balance equation is given by

$$P_{\mathrm{DN}} + P_{\mathrm{WT}} + P_{\mathrm{PV}} = P_{\mathrm{load}} + P^{*}_{\mathrm{cha}} - P_{\mathrm{dis}} \tag{1}$$

where P_{DN} is the overall power generation; P_{WT} is the actual WT power generation; P_{PV} is the actual PV power generation; P_{load} is the base loads within the same distribution network; P^{*}_{cha} is the total load of EV charging; P_{dis} is the total load of EV discharging.

During the charging process, the actual charging power from the supply side is the rated power P^{*}_{cha}; during the discharging process, the actual discharging power P_{dis} is variable.

3.1. WT and PV power generation

In this part, the WT and PV power forecasting models are developed to predict renewable power generation in real-time.

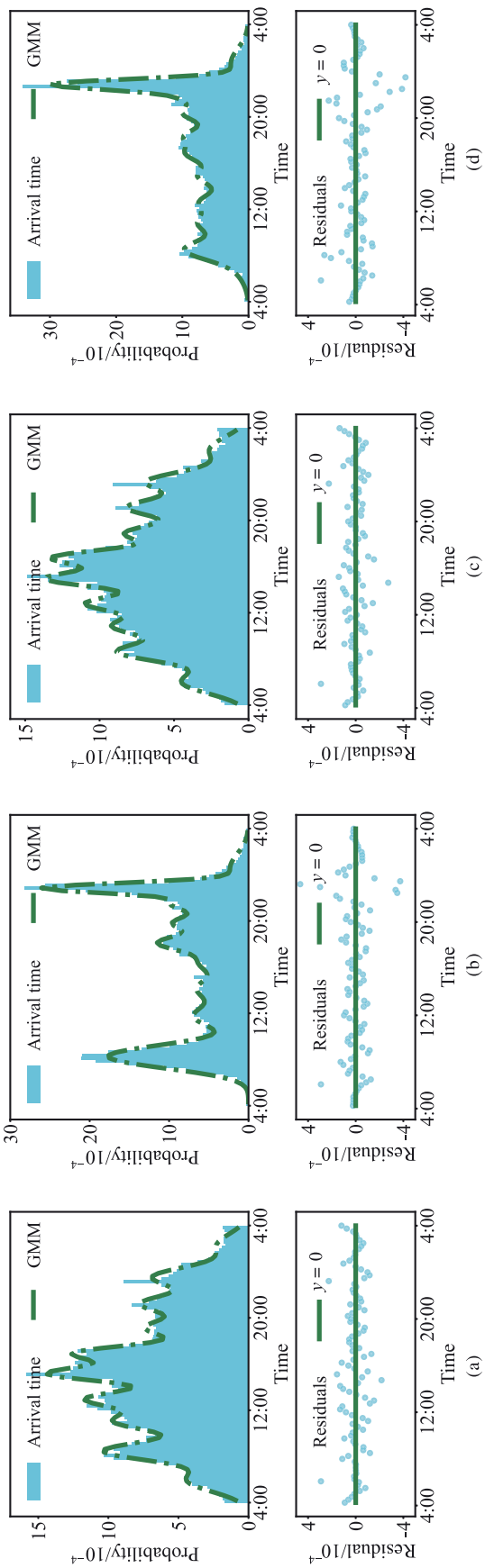

Fig. 3. The distribution of the arrival time of EVs: (a) Fast-charging on weekdays. (b) Slow-charging on weekdays. (c) Fast-charging on weekends. (d) Slow-charging on weekends.

(1) The WT power forecasting model is given by Ref. [20]

$$P_{\mathrm{WT}}^{\mathrm{predicted}}=\begin{cases}0, & v<v_{\mathrm{in}}, v>v_{\mathrm{out}}\\ P_{\mathrm{WT}}^{*}\dfrac{v-v_{\mathrm{in}}}{v^{*}-v_{\mathrm{in}}}, & v_{\mathrm{in}}\le v\le v^{*}\\ P_{\mathrm{WT}}^{*}, & v^{*}\le v\le v_{\mathrm{out}}\end{cases} \tag{2}$$

where $P_{\mathrm{WT}}^{\mathrm{predicted}}$ is the estimated WT output power; v_{in}, v_{out} and v^{*} are the cut-in wind speed, cut-out wind speed, and rated wind speed; P_{WT}^{*} is the rated WT power.

(2) The PV power forecasting model is given by Ref. [35]

$$P_{\mathrm{PV}}^{\mathrm{predicted}}=\eta_{\mathrm{PV}}GA \tag{3}$$

where $P_{\mathrm{PV}}^{\mathrm{predicted}}$ is the estimated PV output power; η_{PV} is the PV conversion efficiency; G is the solar radiation intensity; A is the exposure area.

3.2. The load of EV charging and discharging

P_{EV} is used to represent the total load of EV charging and discharging during time period t, which is given by

$$P_{\mathrm{EV}}=P_{\mathrm{cha}}^{*}-P_{\mathrm{dis}} \tag{4}$$

The relationship between the actual and the rated total power of EV charging and discharging during time period t can be given by

$$P_{\mathrm{cha}}=\eta_{\mathrm{cha}}P_{\mathrm{cha}}^{*} \tag{5}$$

$$P_{\mathrm{dis}}=\eta_{\mathrm{dis}}P_{\mathrm{dis}}^{*} \tag{6}$$

where η_{cha} and η_{dis} are the charging and discharging efficiencies.

The overall charging and discharging powers can be obtained by

$$P_{\mathrm{cha}}=\sum_{n=1}^{n=N}P_{\mathrm{ev,cha}}(n) \tag{7}$$

$$P_{\mathrm{dis}}=\sum_{n=1}^{n=N}P_{\mathrm{ev,dis}}(n) \tag{8}$$

where $P_{\mathrm{ev,cha}}$ and $P_{\mathrm{ev,dis}}$ are the actual charging and discharging powers of the n-th EV. Similarly, each EV satisfies

$$P_{\mathrm{ev,cha}}=\eta_{\mathrm{cha}}P_{\mathrm{ev,cha}}^{*} \tag{9}$$

$$P_{\mathrm{ev,dis}}=\eta_{\mathrm{dis}}P_{\mathrm{ev,dis}}^{*} \tag{10}$$

where $P_{\mathrm{ev,cha}}^{*}$ and $P_{\mathrm{ev,dis}}^{*}$ are the rated charging and discharging powers for a single EV.

3.3. Optimization objectives

The primary control objectives are to mitigate the power fluctuations in the distribution network, reduce charging costs for EV users, and accommodate more renewable energy generation.

(1) Load fluctuation in the distribution network

The total load of the distribution network during the time period t is given by

$$P_{\mathrm{Load}}=P_{\mathrm{load}}+P_{\mathrm{EV}} \tag{11}$$

The Distribution Network Load Fluctuation (DNLF) during the scheduling period can be described as

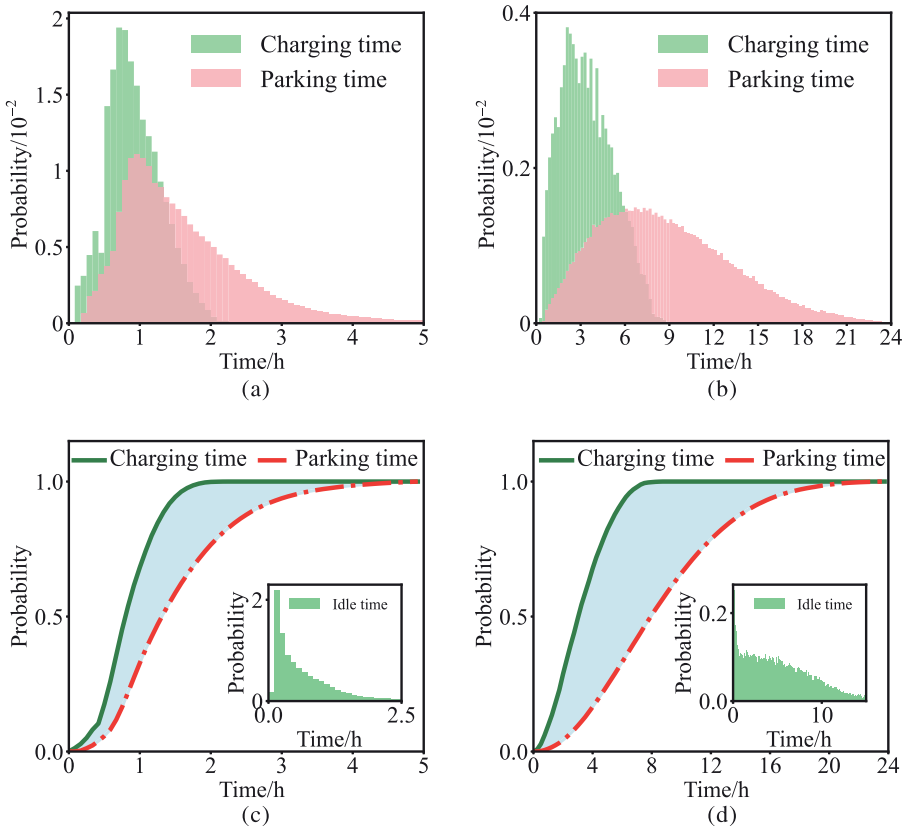

Fig. 4. The distribution of charging and parking time of EVs: (a) Fast charging. (b) Slow-charging. Cumulative probability distribution and idle time distribution of charging and parking time for EVs: (c) Fast-charging. (d) Slow-charging.

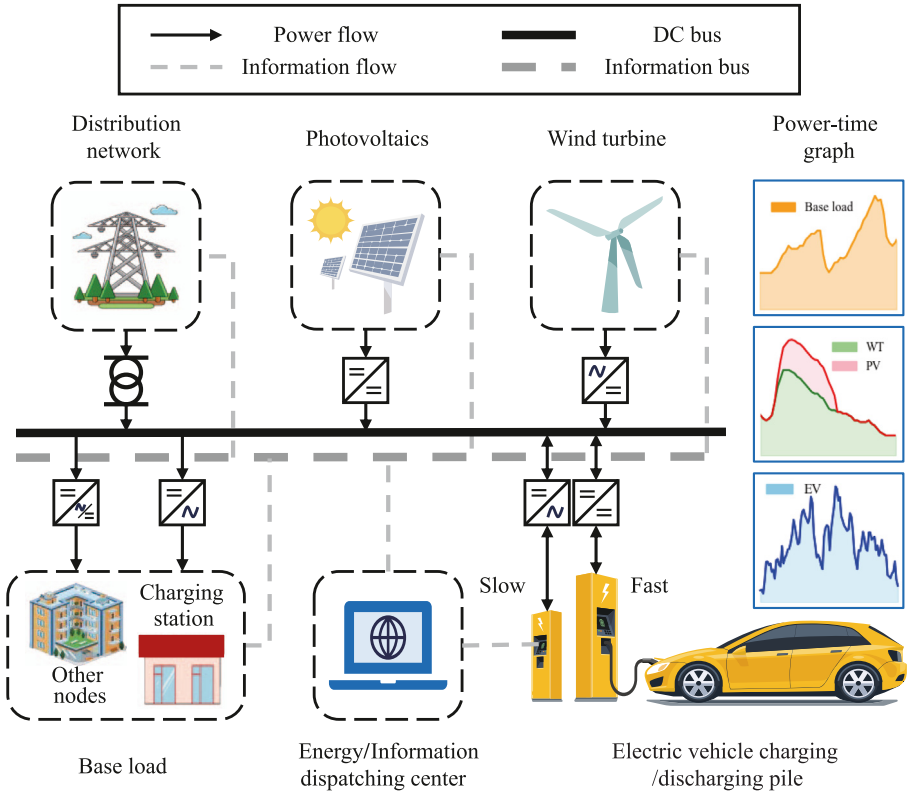

Fig. 5. Illustration of a typical micro-grid with EV charging and renewable energy generation.

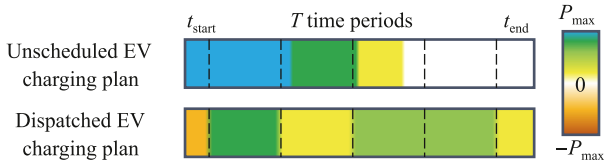

Fig. 6. Comparison between orderly charging and disorderly charging processes.

$$\mathrm{DNLF}=\sqrt{\frac{1}{T}\sum_{t=1}^{t=T}\left(P_{\mathrm{Load}}(t)-\overline{P_{\mathrm{Load}}}\right)^2} \tag{12}$$

where $\overline{P_{\mathrm{Load}}}$ is the average load of the distribution network during the EV charging and discharging processes.

(2) Charging costs of EVs

The charging cost for a single EV during the time period t can be given by

$$C=\gamma_{\mathrm{cha}}P^{*}_{\mathrm{ev,cha}}\Delta t-\gamma_{\mathrm{dis}}P_{\mathrm{ev,dis}}\Delta t \tag{13}$$

where γ_{cha} and γ_{dis} are the real-time charging and discharging prices. Since an EV is either in the charging or discharging mode at a specific time, it must satisfy

$$P^{*}_{\mathrm{ev,cha}}\cdot P_{\mathrm{ev,dis}}=0 \tag{14}$$

Then the Electric Vehicle Charging Cost (EVCC) over T scheduling periods can be described as

$$\mathrm{EVCC}=\sum_{t=1}^{t=T}C(t) \tag{15}$$

(3) Real-time energy consumption difference

The powers generated by the WT and PV systems cannot be accurately predicted. P_{diff} is defined as the difference between the forecast renewable energy generation and the EV charging and discharging power during time period t, which is given by

$$P_{\mathrm{diff}}=\left|P_{\mathrm{EV}}-\left(P^{\mathrm{predicted}}_{\mathrm{PV}}+P^{\mathrm{predicted}}_{\mathrm{WT}}\right)\right| \tag{16}$$

To maximize the utilization of renewable energy generation, the EV charging and discharging load curve should closely match the predicted renewable power generation. This can be achieved by minimizing the Real-time Energy Consumption Difference (RECD), which is given by

$$\mathrm{RECD}=\frac{1}{T}\sum_{t=1}^{t=T}P_{\mathrm{diff}}(t) \tag{17}$$

3.4. Constraints

(1) The capacity of the distribution equipment

In time period t, the total load of the distribution network should be within the capacity range of the distribution equipment, which can be expressed as

$$P^{-}_{\mathrm{MTF}}\le P_{\mathrm{DN}}\le P^{+}_{\mathrm{MTF}} \tag{18}$$

where P^{+}_{MTF} and P^{-}_{MTF} are the maximum charging and discharging powers that the distribution equipment can withstand.

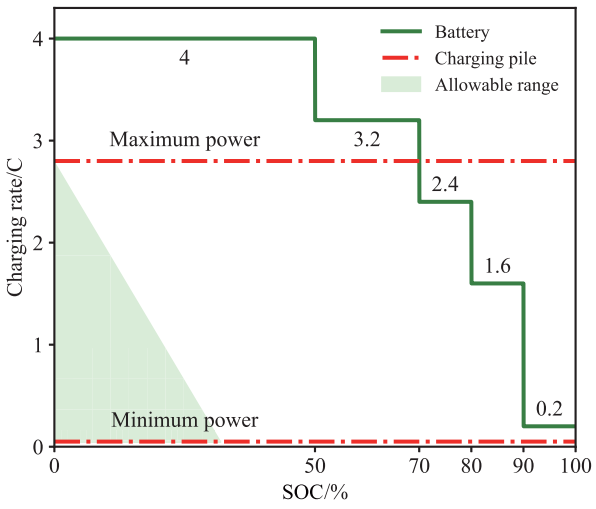

Fig. 7. Illustration of the multi-stage constant-current charging process.

(2) The output power of MG

The WT and PV output power limits are described as

$$0\le P^{\mathrm{predicted}}_{\mathrm{WT}}\le P^{*}_{\mathrm{WT}} \tag{19}$$

$$0\le P^{\mathrm{predicted}}_{\mathrm{PV}}\le P^{*}_{\mathrm{PV}} \tag{20}$$

The relationship between the charging and discharging powers of EVs and the charging and discharging powers of charging piles is given by

$$P_{\mathrm{ev,cha}}=\eta_{\mathrm{cha}}P_{\mathrm{pile,cha}} \tag{21}$$

$$P_{\mathrm{ev,dis}}=\frac{1}{\eta_{\mathrm{dis}}}P_{\mathrm{pile,dis}} \tag{22}$$

The multi-stage constant current charging method is often employed for fast charging control [52], as shown in Fig. 7. The power boundaries for fast charging during time period t can be given by

$$\eta_{\mathrm{cha}}P^{\mathrm{min}}_{\mathrm{pile,cha}}\le P_{\mathrm{ev,cha}}\le\min\left(\eta_{\mathrm{cha}}P^{\mathrm{max}}_{\mathrm{pile,cha}},P^{\mathrm{c-c}}_{\mathrm{cha}}\right) \tag{23}$$

$$\frac{1}{\eta_{\mathrm{dis}}}P^{\mathrm{min}}_{\mathrm{pile,dis}}\le P_{\mathrm{ev,dis}}\le\min\left(\frac{1}{\eta_{\mathrm{dis}}}P^{\mathrm{max}}_{\mathrm{pile,dis}},P^{\mathrm{c-c}}_{\mathrm{dis}}\right) \tag{24}$$

For slow-charging, the Alternating Current charging rate is generally less than 0.2 C, which can be given by

$$\eta_{\mathrm{cha}}P^{\mathrm{min}}_{\mathrm{pile,cha}}\le P_{\mathrm{ev,cha}}\le\eta_{\mathrm{cha}}P^{\mathrm{max}}_{\mathrm{pile,cha}} \tag{25}$$

$$\frac{1}{\eta_{\mathrm{dis}}}P^{\mathrm{min}}_{\mathrm{pile,dis}}\le P_{\mathrm{ev,dis}}\le\frac{1}{\eta_{\mathrm{dis}}}P^{\mathrm{max}}_{\mathrm{pile,dis}} \tag{26}$$

where $P^{\mathrm{min}}_{\mathrm{pile,cha}}$ and $P^{\mathrm{min}}_{\mathrm{pile,dis}}$ are the minimum charging and discharging powers to sustain charging/discharging sessions, and 0.2 kW is adopted in this study; $P^{\mathrm{max}}_{\mathrm{pile,cha}}$ and $P^{\mathrm{max}}_{\mathrm{pile,dis}}$ are the maximum charging and discharging powers of the charging piles, and it is assumed that

$$P^{\mathrm{max}}_{\mathrm{pile,cha}}=P^{\mathrm{max}}_{\mathrm{pile,dis}} \tag{27}$$

where $P^{\mathrm{c-c}}_{\mathrm{cha}}$ and $P^{\mathrm{c-c}}_{\mathrm{dis}}$ are the upper bounds of the charging and discharging power in the multi-stage constant-current charging operation.

(3) SOC

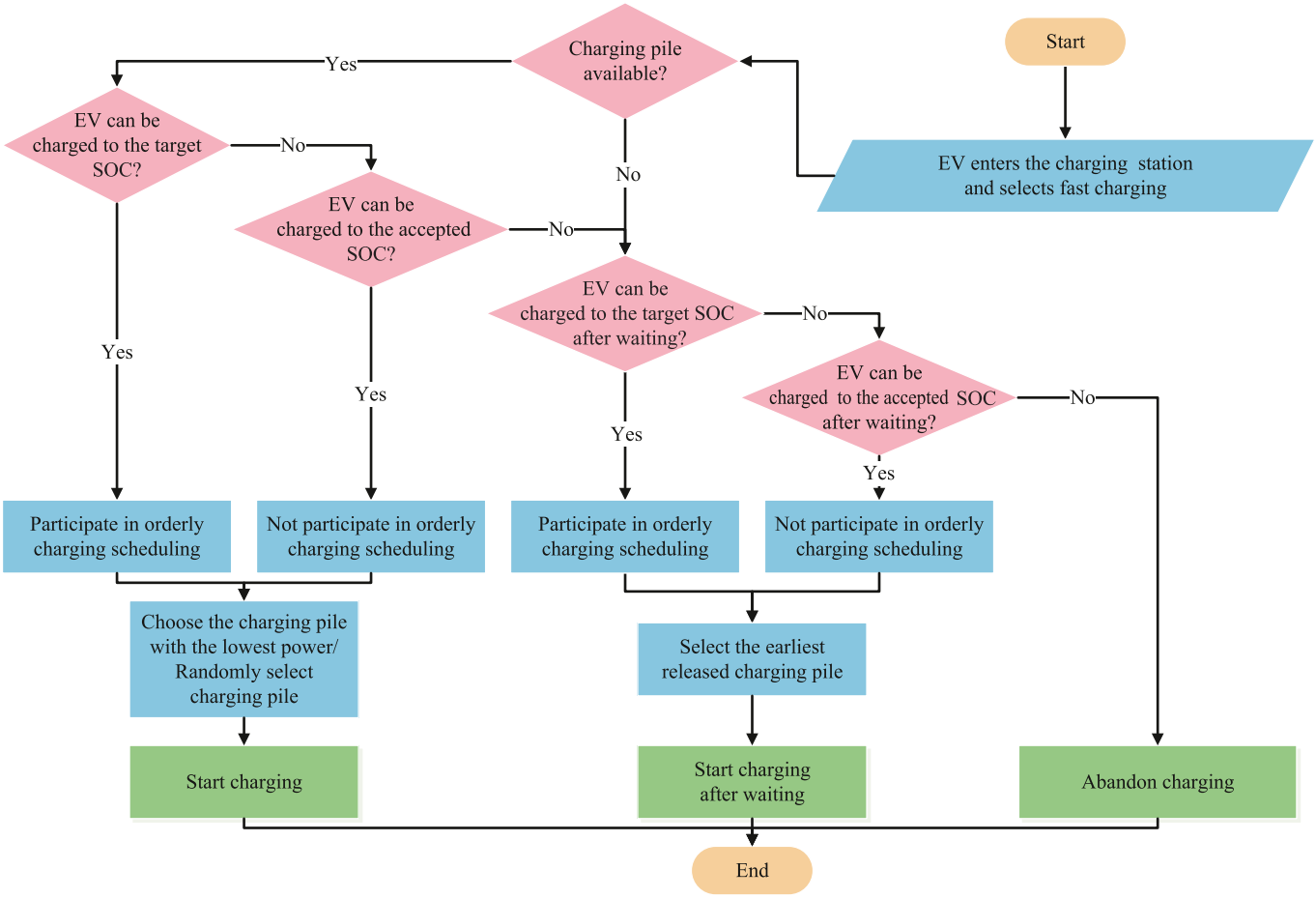

Fig. 8. Flowchart of the proposed EV fast-charging pile allocation method.

Throughout the entire process of EV charging and discharging operations, it should meet

$$0 \le \mathrm{SOC}_{\mathrm{ev}} \le 100\% \tag{28}$$

The variation of SOC for a single EV between adjacent time periods can be described as

$$\mathrm{SOC}(t) = \mathrm{SOC}(t-1) + \frac{P_{\mathrm{ev,cha}}\Delta t}{E_{\mathrm{ev}}} - \frac{P^{*}_{\mathrm{ev,dis}}\Delta t}{E_{\mathrm{ev}}} \tag{29}$$

where E_{ev} is the battery capacity.

The overall SOC variation can be given by

$$\mathrm{SOC}_{\mathrm{ev,end}} = \mathrm{SOC}_{\mathrm{ev,start}} + \frac{\Delta t}{E_{\mathrm{ev}}} \sum_{t=t_{\mathrm{start}}}^{t=t_{\mathrm{end}}} \left(P_{\mathrm{ev,cha}}(t) - P^{*}_{\mathrm{ev,dis}}(t) \right) \tag{30}$$

where $\mathrm{SOC}_{\mathrm{ev,\ start}}$ and $\mathrm{SOC}_{\mathrm{ev,end}}$ are the start and end SOCs; t_{start} and t_{end} are the start and end time. It is evident that the power during the start and end periods satisfies

$$P^{\mathrm{real}}_{\mathrm{ev,start}} t_{\mathrm{start}} = P_{\mathrm{ev,start}} \Delta t \tag{31}$$

$$P^{\mathrm{real}}_{\mathrm{ev,end}} t_{\mathrm{end}} = P_{\mathrm{ev,end}} \Delta t \tag{32}$$

$$0 < t_{\mathrm{start}}, t_{\mathrm{end}} \le \Delta t \tag{33}$$

where $P^{\mathrm{real}}_{\mathrm{ev,start}}$ and $P^{\mathrm{real}}_{\mathrm{ev,end}}$ are the actual powers at the start and end periods; $P_{\mathrm{ev,start}}$ and $P_{\mathrm{ev,end}}$ are the average powers at the start and end periods.

$$\mathrm{SOC}_{\mathrm{ev,accepted}} = \mathrm{SOC}_{\mathrm{ev,start}} + 0.8 \times \left(\mathrm{SOC}_{\mathrm{ev,expected}} - \mathrm{SOC}_{\mathrm{ev,start}} \right) \tag{34}$$

where $\mathrm{SOC}_{\mathrm{ev,\ expected}}$ is the expected end SOC after charging completion. The used NSGA-II algorithm inevitably results in a difference between $\mathrm{SOC}_{\mathrm{ev,end}}$ and $\mathrm{SOC}_{\mathrm{ev,\ expected}}$, which is given by

$$\mathrm{SOC}_{\mathrm{error}} = \left| \mathrm{SOC}_{\mathrm{ev,end}} - \mathrm{SOC}_{\mathrm{ev,expected}} \right| \tag{35}$$

The error should be maintained within a certain range, which is given by

$$\mathrm{SOC}_{\mathrm{error}} \le 0.1\% \tag{36}$$

4. Control strategy

To enhance the operational efficiency of the charging station, charging piles are first allocated to the arriving EVs, and then charging scheduling is implemented.

4.1. Charging pile allocation

Fast charging piles with different maximum powers are installed at the charging station, while all slow charging piles have the same maximum power. To efficiently allocate charging piles to the arriving EVs, a Minimum Power Allocation Method (F-MPAM) and a Random Power Allocation Method (F-RPAM) are proposed for fast-charging EVs, and the Random Power Allocation Method (S-RPAM) is presented for slow-charging EVs. Several assumptions are made for simplification:

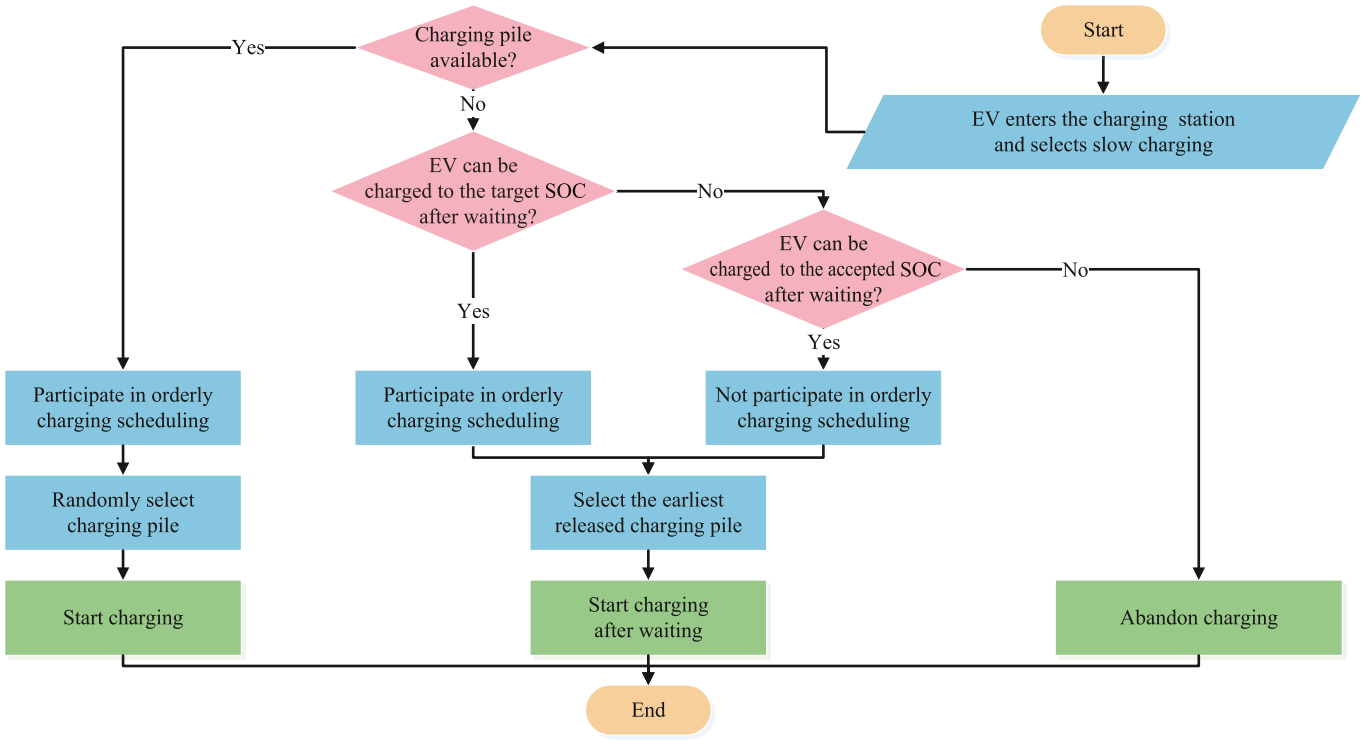

Fig. 9. Flowchart of the proposed EV slow-charging pile allocation method.

- EVs opting for fast charging will not be assigned to slow-charging piles, and EVs opting for slow charging will not be assigned to fast-charging piles.
- There is always a charging pile capable of fulfilling the charging demands when all the charging piles are available at the station.
- The actual departure time is consistent with the estimated departure time.
- The time waiting for an available charging pile is not excessively long, and the longest waiting time satisfies

$$t_{\text{wait}} = \min(0.3 \times t_{\text{park}}, 60) \tag{37}$$

where t_{wait} is the waiting time and t_{park} is the expected stay time.

EVs are assumed not to participate in charging scheduling in the following situations:

- The EV's expected end SOC is below 80%.
- The expected parking time is less than Δt and the parking period falls within the same time period.

(1) F-MPAM and F-RPAM

Fig. 8 shows the F-MPAM and F-RPAM methods proposed in this study. The specific steps are as follows:

Step 1: After the vehicle enters the charging station, the EV owner interacts with the EIDC to obtain information about the current SOC, expected end SOC, minimum accepted SOC upon departure, and estimated departure time.

Step 2: If charging piles are available, identify all the charging piles capable of realizing the expected end SOC.

Step 3: If there are charging piles available, the EV participates in charging scheduling. The charging pile with the lowest power output is assigned to the EV (F-MPAM), or a charging pile that meets the conditions is randomly selected and assigned to the EV (F-RPAM), and the charging operation begins.

Step 4: If there are no such piles available, identify all the charging piles capable of reaching the accepted end SOC.

Step 5: If such piles exist, the EV opts for charging with the maximum power throughout the charging process and will not participate in charging scheduling. The charging pile with the lowest power output is assigned to the EV, or a randomly selected pile meeting the criteria is assigned to the EV, and the charging operation begins.

Step 6: If there are no such piles available, identify all the piles with which the EV can still reach its target end SOC after waiting for some time.

Step 7: If such piles exist, the EV opts to participate in charging scheduling. The first available charging pile is assigned to the EV.

Step 8: If there are no such piles available, identify all the piles with which the EV can reach the accepted SOC after waiting.

Step 9: If such piles exist, the EV does not participate in charging scheduling. The earliest released charging pile is assigned to the EV, and the charging operation begins after waiting.

Step 10: If no such piles exist, the EV abandon charging.

Step 11: If charging piles are unavailable, go back to Step 6 to Step 10.

When not assigning charging piles (NA), if the EV does not know when the charging pile will be released and no piles are available, the EV immediately abandons charging. After completing Step 1 to Step 5, charging is abandoned directly. Additionally, in Step 3 and Step 5, the EV randomly selects a charging pile.

(2) S-RPAM

Fig. 9 shows the S - RPAM method proposed in this section. The specific steps are as follows:

Step 1: After the vehicle for slow charging enters the charging station, the EV owner interacts with the EIDC to obtain the EV's current SOC, expected SOC at departure, minimum accepted SOC at departure, and expected departure time from the charging station.

Step 2: If a charging pile is available, the EV participates in charging scheduling. A charging pile is randomly assigned to the EV, and the charging operation begins.

Step 3: If no charging pile is available, obtain all the piles that will be available before the EV's departure time and can charge the EV to the expected SOC after being available.

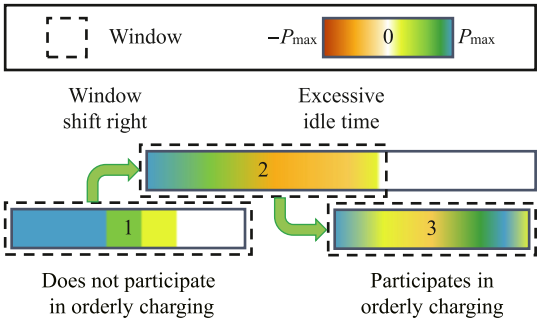

Fig. 10. Illustration of the sliding window mechanism.

Step 4: If such piles exist, the EV participates in charging scheduling. The earliest available charging pile is assigned to the EV, and the EV waits before starting to charge.

Step 5: If no such piles exist, obtain all the piles that can charge the EV to the minimum accepted SOC after being available.

Step 6: If such piles exist, the EV does not participate in charging scheduling. The earliest available charging pile is assigned to the EV, and the EV waits before starting to charge.

Step 7: If no such piles exist, the EV has to give up charging.

When not performing charging pile allocation (NA), if no charging pile is available, the EV immediately gives up charging.

4.2. Sliding window mechanism for orderly charging

This section presents a charging scheduling strategy based on a sliding window mechanism. The NSGA-II and Entropy-TOPSIS methods are utilized to formulate an efficient charging schedule for each EV. To verify the superiority of the proposed method, a comparison study with disorderly charging is carried out.

Charge as soon as possible (ASAP): Once the EV is connected to a charging pile, it immediately adopts a multi-stage constant-current fast-

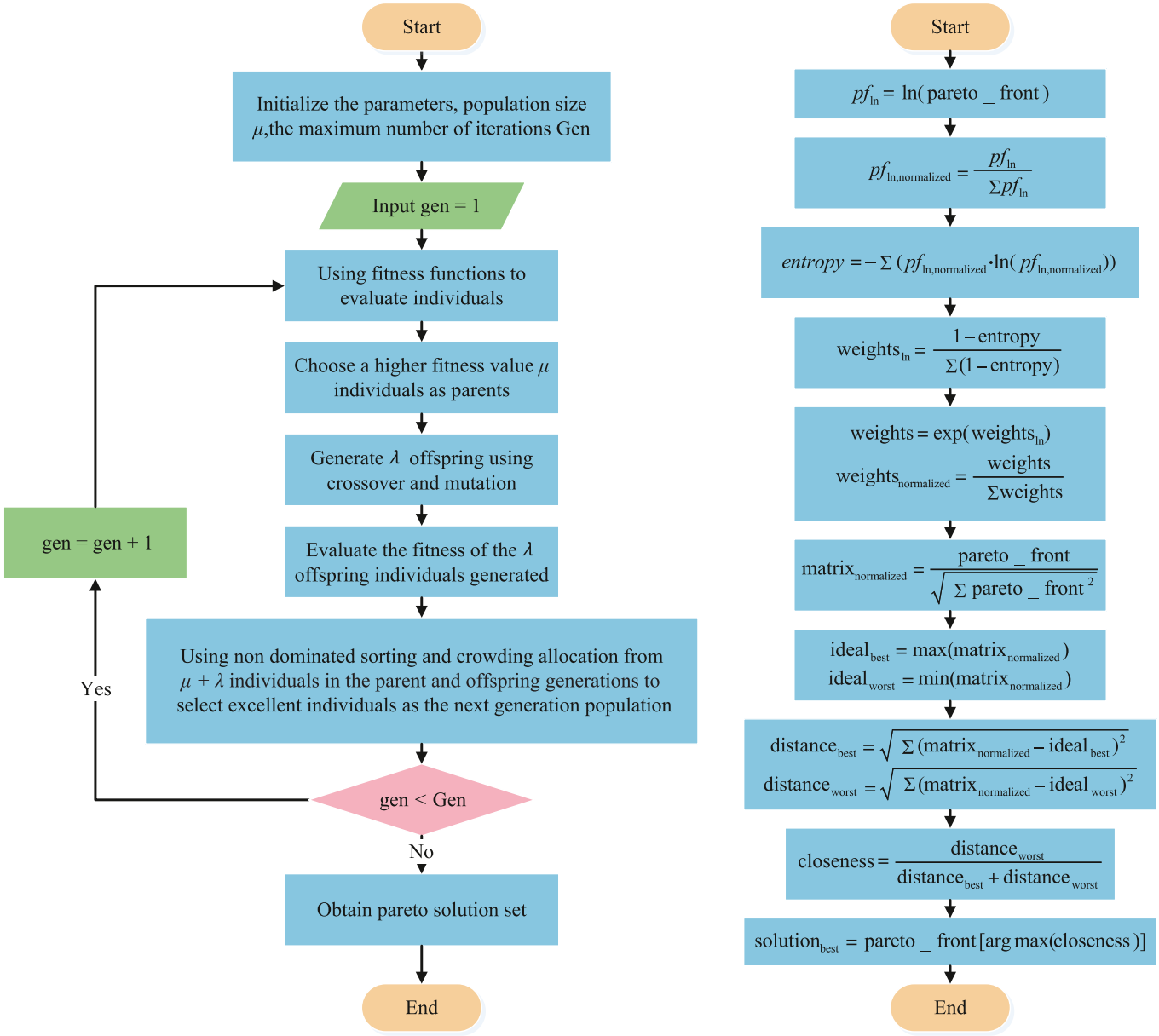

Fig. 11. Flowcharts of the NSGA-II and Entropy-TOPSIS algorithms.

charging regime to fulfill the charging demand within the charging power limits described in Eqs. (23) and (24).

Orderly charging: After the EV is connected to a charging pile, the EIDC formulates a charging schedule based on the charging demand. It is worth noting that the EVs under charging operations will not be affected. The general charging scheduling procedures are as follows:

Step 1: The EV starts the charging operation, and the length of the scheduling window is determined.

Step 2: The EV determines whether to participate in charging scheduling.

Step 3: If the vehicle chooses to participate in charging scheduling, a charging schedule is derived.

Step 4: If the vehicle does not choose to participate in charging scheduling, ASAP is activated.

Step 5: Slide the window and repeat Steps 1 to 4.

As shown in Fig. 10, EV 1 chooses not to participate in charging scheduling, while EVs 2 and 3 do. EV 2 has a long idle time and the scheduling window length is shorter than the EV's parking duration. For fast charging, it is assumed that the scheduling duration satisfies

$$t_{\text{dispatch}} = \min(t_{\text{park}}, t_{\text{ASAP}} + 120) \tag{38}$$

For slow charging, the scheduling duration satisfies

$$t_{\text{dispatch}} = \min(t_{\text{park}}, t_{\text{ASAP}} + 240) \tag{39}$$

where t_{dispatch} is the scheduling window length; t_{park} is the EV's parking duration; t_{ASAP} is the time required for the EV to charge to the expected SOC under the ASAP charging strategy, which is derived by

$$t_{\text{ASAP}} = E_{\text{ev}} \sum_{i=0}^{i=I} \frac{\text{SOC}_{i+1} - \text{SOC}_i}{P_{\text{cha},i}^{\max}} \tag{40}$$

where I is the number of SOC stage changes, with a maximum value of 4; $P_{\text{cha},i}$ is the maximum charging power in the i-th stage, satisfying

$$\text{SOC}_0 = \text{SOC}_{\text{ev,start}} \tag{41}$$

$$\text{SOC}_{I+1} = \text{SOC}_{\text{ev,expected}} \tag{42}$$

$$P_{\text{cha},i}^{\max} = \min(\eta_{\text{cha}} P_{\text{pile,cha}}^{\max}, P_{\text{cha}}^{\text{c-c}}) \tag{43}$$

The limitation on the scheduling duration has the following benefits:

- It reduces the number of decision variables, thereby lowering computational power requirements.
- It reduces the fire hazard caused by EVs being connected to charging piles for extended periods [53].
- It avoids low end SOCs due to EV owners leaving earlier than expected.

Combining the orderly charging scheduling method, the decision variables are given by

$$[P_{\text{ev}}^1, P_{\text{ev}}^2, \cdots P_{\text{ev}}^t, \cdots P_{\text{ev}}^T] \tag{44}$$

where P_{ev}^t is the charging and discharging power of the EV in the t-th time period, and its value should satisfy the constraints of Eqs. (23)–(26).

4.3. Optimization methods

In this section, the NSGA-II algorithm is employed to obtain the Pareto-front solutions of the scheduling model, and the Entropy-TOPSIS method is utilized to determine the optimal solution.

(1) The modified NSGA-II algorithm

Table 3
Specifications of the fast and slow charging piles.

Pile type	Pile power/kW	Number
F–C	120	2
	45	35
	37.5	5
	31.5	8
S–C	7	102

Table 4
TOU electricity price in Beijing.

Period	Peak	Normal	Valley
Time	10:00–15:00	07:00–10:00	00:00–07:00
	16:00–17:00	15:00–16:00	23:00–24:00
	18:00–21:00	17:00–18:00	
		21:00–23:00	
$\text{Price}_{\text{cha}}$	1.468,3	1.044,2	0.661,9
$\text{Price}_{\text{dis}}$	1.200,0	1.200,0	1.200,0

Table 5
The number of EVs arriving at the charging station every day.

Day	Mon	Tue	Wed	Thu	Fri	Sat	Sun
F–C	253	279	274	278	243	292	274
S–C	35	41	47	38	38	44	36

Table 6
Parameters of the WT and PV forecasting models.

Parameter	v_{in}/(m·s^{-1})	v_{out}/(m·s^{-1})	v^*/(m·s^{-1})	P_{WT}/kW	η_{PV}	A/m^2
Value	3	25	12	300	0.25	300

Table 7
Parameters of the used NSGA-II algorithm.

Parameter	Value	Parameter	Value
μ	50	λ	100
Iterations	200	Population	50
Crossover rate	0.7	Mutation rate	0.2

A modified NSGA-II algorithm based on the $\mu+\lambda$ evolution is employed in this study. It has the advantages of maintaining population diversity, improving search efficiency and convergence speed, and offering flexibility and adaptability for solving various optimization problems. μ and λ are the two key parameters representing the numbers of the selected individuals and generated offsprings. Their roles in the optimization-derivation process are illustrated in Fig. 11.

(2) Entropy-TOPSIS

The Entropy-TOPSIS method is a multi-criteria decision-making approach based on the information entropy and TOPSIS. By calculating the entropy between multiple attributes, it avoids the adverse influence of subjective weight assignment on the ranking results. TOPSIS determines the best solution by calculating the distance between the weighted ideal and negative ideal solutions. The computation process is illustrated in Fig. 11.

5. Results

This section focuses on the following aspects based on the scenario depicted in Fig. 5: the impact of different charging pile allocation mechanisms on EV charging behaviors and the effects of EV participation

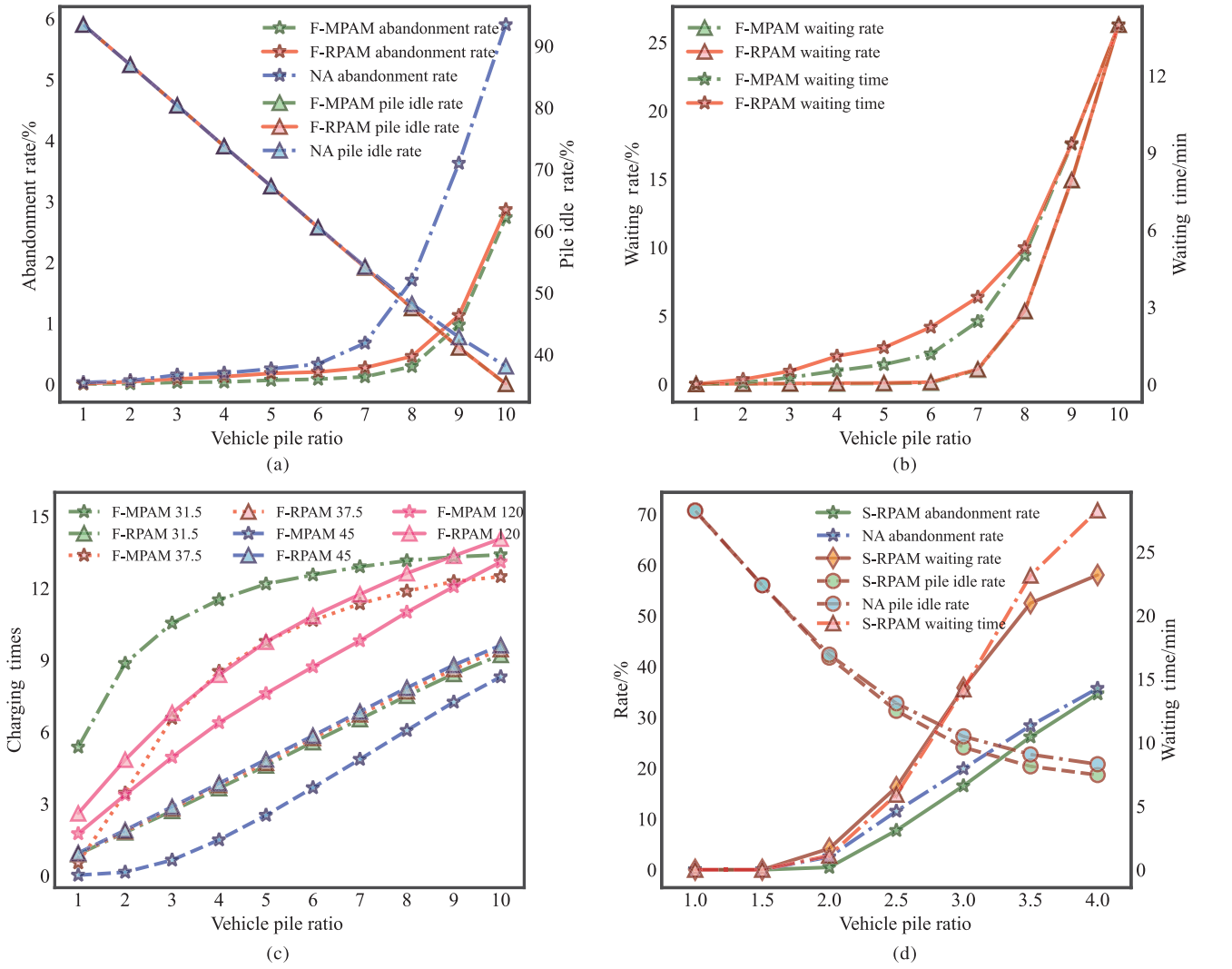

Fig. 12. The results undert the proposed charging pile allocation mechanism: (a) Fast-charging abandonment rate and pile idle rate. (b) Fast-charging waiting rate and average waiting time. (c) Fast charging pile usage. (d) Slow-charging abandonment rate, waiting rate, average waiting time, and pile idle rate.

in charging scheduling on optimization objectives under various scenarios. The following assumptions are made:

- Each EV is assumed to interact with the charging station in a single interaction, and the number of charging piles with different power levels at the charging station remains fixed in different time periods.
- It is assumed that EV owners will not change their charging plans abruptly and will comply with the charging schedule. The expected charging energy meets their next trip's requirements.
- It is assumed that the base load of the grid and the renewable energy generation in different time periods are known, and the power supply is not affected by spontaneous events.
- The model only considers the EV's behaviors on the time scale and ignores the potential impact of traffic conditions around the charging station [54].

Simulation studies were conducted on a computer equipped with an AMD Ryzen 9 7945HX CPU. The abbreviations used are presented in Table 2.

5.1. Case studies

This study takes the Lucheng charging station in Beijing as the research object. The capacity of the distribution transformer is 17,760 kVA. It is assumed that all the charging piles have a charging/discharging efficiency of 0.98. The default simulation time step is 15 min, i.e., $\Delta t = 15$.

The number of the charging piles and the TOU electricity prices are shown in Tables 3 and 4.

Based on real data statistics, the number of EV arrivals at the Lucheng charging station each day within one week is shown in Table 5.

Considering the location of the Lucheng charging station, the parameters for the WT and PV generation are listed in Table 6.

The real-time wind speed v and the direct normal irradiation G were referenced from San Francisco, USA, which has a similar latitude as Beijing. The parameters of NSGA-II are listed in Table 7.

Five charging scheduling scenarios are considered:

Scenario 0: Disorderly charging.

Scenario 1: No renewable energy generation and no V2G.

Scenario 2: Renewable energy generation and no V2G.

Scenario 3: No renewable energy generation but V2G.

Scenario 4: Renewable energy generation and V2G.

5.2. Simulation results

5.2.1. Comparison of charging pile allocation mechanisms

To quantitatively assess the effectiveness of the charging pile allocation algorithms, simulations were conducted using the TOU electricity

Table 8
Specifications of E.

Parameter	Value	Parameter	Value
$SOC_{ev,\ start}$/%	36	$SOC_{ev,\ expected}$/%	100
E_{ev}/kWh	60	$P^{max}_{pile,cha}$/kW	45
η_{cha}/η_{dis}	0.98	t_{park}/min	124

price data in Beijing, as presented in Table 3. The evaluation metrics considered include the charging waiting time, charging abandonment rate, pile idle rate, waiting rate, average waiting time, and charging times under different vehicle-to-pile ratios. The definitions of these metrics are as follows:

- Vehicle-to-pile ratio: The ratio of the number of EVs charging at the station to the number of charging piles.
- Charging abandonment rate: The proportion of EVs that leave the station without charging relative to the total number of arriving EVs.
- Pile idle rate: The ratio of the total idle time of charging piles in a day to the total operating time of the station in a day.
- Waiting rate: The ratio of the number of EVs waiting to charge to the number of EVs currently being charged.
- Average waiting time: The mean time an EV spends waiting for a charging pile to become available.
- Charging times: The average number of charging sessions a charging pile experiences in a day.

The charging abandonment rate, waiting rate, average waiting time, and pile idle rate for fast charging are illustrated in Fig. 12(a) and (b). With the increasing vehicle-to-pile ratio, the first three metrics exhibit noticeable increase while the pile idle rate sees an explicit decline. This indicates that a high vehicle-to-pile ratio may lead to a higher charging abandonment rate and longer waiting time, despite reducing the pile idle rate. The former undermines the customer satisfaction with the charging service, while the latter can enhance the charging station's operational efficiency. Thus, it is essential to strike a balance between them. According to the data, an ideal fast-charging vehicle-to-pile ratio of around 7 can balance the charging abandonment and pile idle rate. The statistical data in Table 5 show that the actual fast-charging vehicle-to-pile ratio of the studied charging station is between 5 and 6, suggesting its potential to accommodate more EV charging demands.

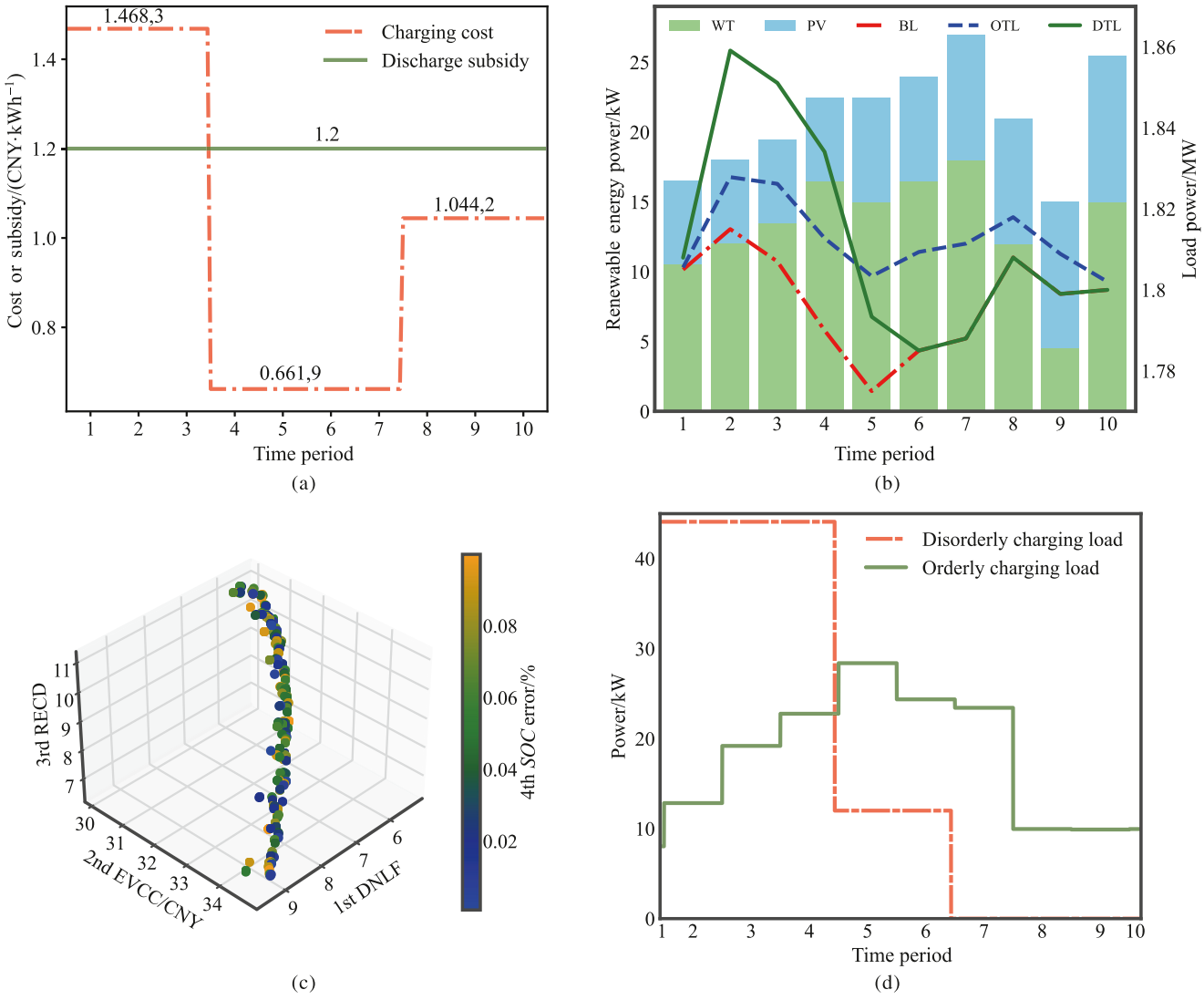

Fig. 13. Single EV regulation results: (a) Charging and discharging prices during the parking period; (b) Renewable energy generation, base load, and total load of the distribution network during the parking period with and without charging scheduling; (c) The Pareto front; (d) Charging and discharging powers with and without charging scheduling.

Table 9
The comparison of various indicators. $T = 10$.

Objective	DNLF	EVCC	RECD	SE
D-C	24.96	43.79	20.25	0
O–C	8.63	34.12	7.09	0.096%

Compared with the NA method, the F-MPAM and F-RPAM methods can remarkably reduce the charging abandonment rate, demonstrating the effectiveness of the proposed allocation schemes. Under high vehicle-to-pile ratios, the pile idle rate slightly decreases. The reason for the negligible effect under low vehicle-to-pile ratios is that the pile idle rate mainly depends on actual EV stay duration. In low-ratio scenarios, the stay times of the three methods are similar. In high-ratio scenarios, the

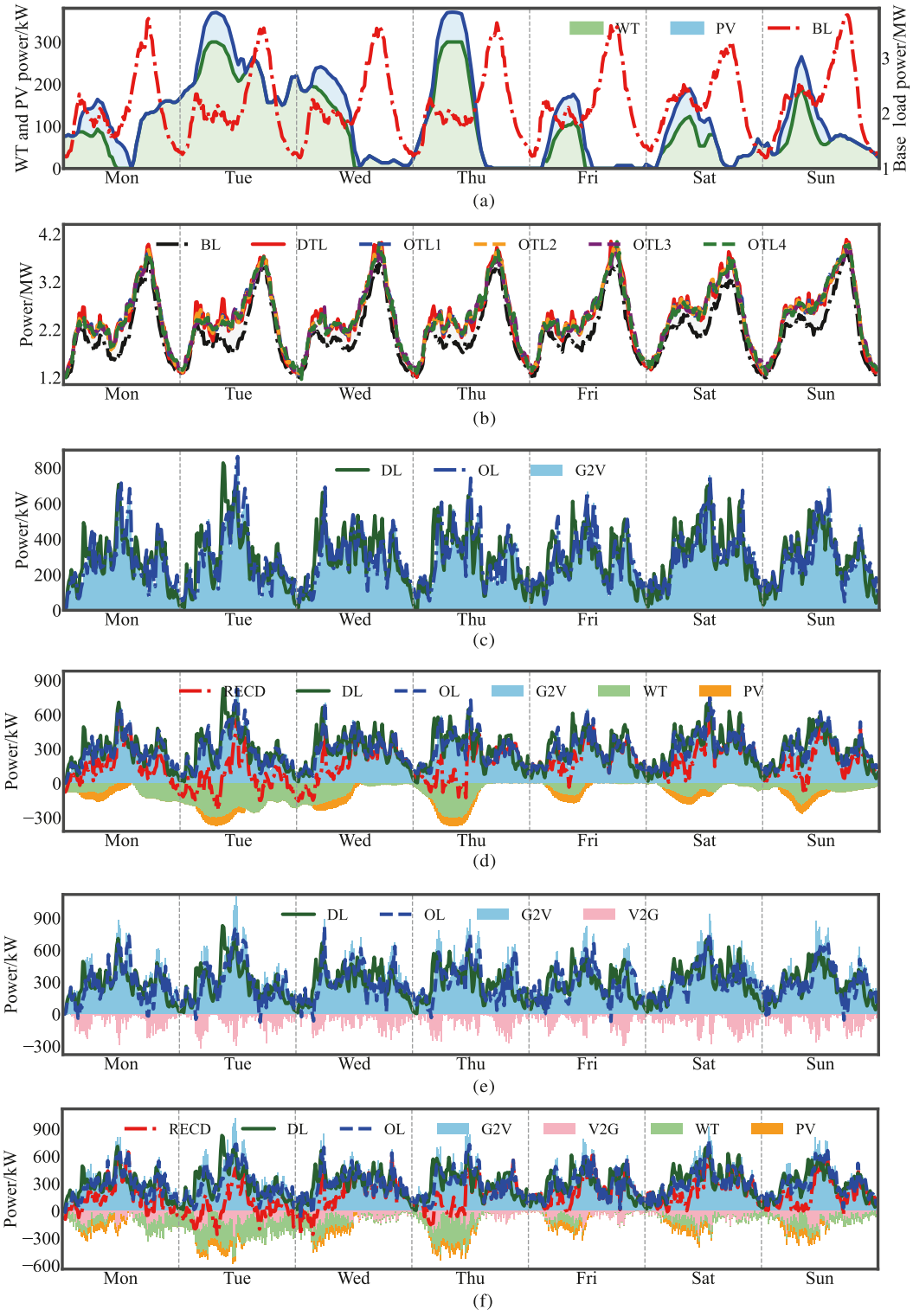

Fig. 14. Weekly simulation results: (a) Basic load and renewable energy generation power, (b) Comparison of the total load of orderly charging throughout the week in different scenarios, (c) Scenario 1, (d) Scenario 2, (e) Scenario 3, (f) Scenario 4.

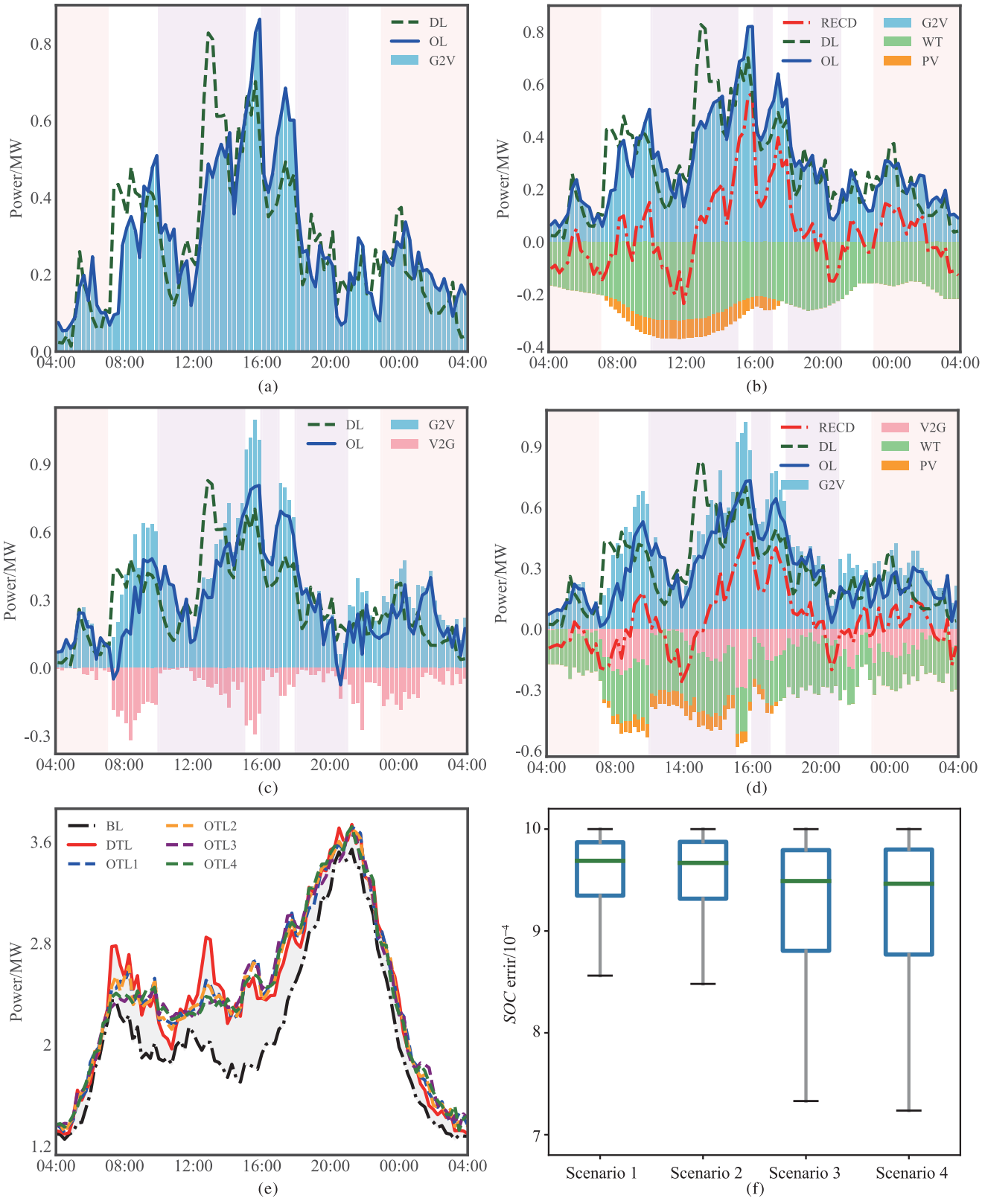

Fig. 15. Simulation results for Tuesday: (a) Scenario 1; (b) Scenario 2; (c) Scenario 3; (d) Scenario 4; (e) Comparison of distribution network load under orderly and disorderly charging; (f) SOC error.

NA method abandons charging without waiting for an idle pile, while F-MPAM and F-RPAM reduce the pile idle rate as EVs are willing to wait. Compared with F-RPAM, F-MPAM has a slightly lower abandonment rate and average waiting time while maintaining a similar pile idle rate. This is because F-MPAM prefers using slow-charging piles for some EVs, leaving more fast-charging piles available. The usage of fast - charging piles for fast-charging EVs is depicted in Fig. 12(c). F-RPAM shows a more uniform preference for all the charging piles. Frequent use of charging piles can reduce their lifespans [55]. In an orderly charging scenario, EVs are expected to have sufficient idle time for load shifting. F-MPAM makes some EVs originally opting for high-power charging choose low-power charging, reducing their idle time and potentially limiting their participation in charging scheduling. Therefore, from the EV user's perspective, F-MPAM slightly reduces the abandonment rate and average waiting time. From the charging station's perspective, F-MPAM may compromise the potential for EVs to participate in charging scheduling. Thus, the F-RPAM method is more suitable for the Lucheng charging station, while the F-MPAM method may have better feasibility when vehicle-to-pile ratios are relatively high.

The abandonment rate, waiting rate, average waiting time, and pile idle rate of slow-charging EVs are shown in Fig. 12(d). With the increasing vehicle-to-pile ratio, these metrics change in a similar pattern to fast-charging EVs under the S-RPAM method. When the vehicle -to-pile ratio is fixed, the abandonment rate under S-RPAM is significantly lower than that under NA. When the ratio exceeds 1.5, the first three metrics start to increase while the pile idle rate decreases. Therefore, the S-RPAM method can effectively balance the operating costs of the charging station and the satisfaction of EV users, and thus it is adopted as the charging pile allocation algorithm for slow-charging EVs in subsequent simulation studies. For the Lucheng charging station, the ideal slow-charging vehicle-to-pile ratio is around 1.5, while its actual ratio is less than 0.5.

The charging pile allocation mechanism can significantly improve the operational efficiency of charging stations. The abandonment rate, charging waiting rate, average charging waiting time, charging pile idle rate, and charging pile usage can serve as efficient indicators for comprehensively evaluating charging station operations [56]. For a charging station with limited charging capacity, the charging pile allocation mechanism is essential for unleashing the potential of charging scheduling.

5.2.2. *Charging scheduling results*

(1) Scheduling results for one EV

Analyzing the scheduling results for a single EV provides valuable insights into the optimization approach. Consider an EV with the basic information presented in Table 8, operating within a 10-time-slot period with no other EVs charging simultaneously. In reality, the actual charging/discharging efficiency of EVs can be influenced by factors such as battery temperature [57]. However, due to the lack of relevant data, fixed values were utilized in the simulation. The charging and discharging prices, base load, and forecast renewable energy generation are illustrated in Fig. 13(a) and (b).

Upon receiving the EV's information, EIDC employs the NSGA-II algorithm to obtain the Pareto-front solution set. Then the Entropy-TOPSIS method is utilized to determine the optimal charging schedule for the EV. Fig. 13(c) depicts the Pareto-front, and Fig. 13(d) shows the comparison between the optimal charging schedule and the disorderly charging load. The total load comparison is presented in Fig. 13(b). The process of obtaining the EV information and deriving the optimal charging schedule takes approximately 2.01 s.

A comparison of various indicators is presented in Table 9. It is evident that the proposed scheduling method leads to remarkable reductions in total load fluctuation, user charging cost, and renewable energy curtailment.

Table 10
The participation rate of orderly charging for the entire week.

EVN	POCN	ACN	WCN	FSN
2,172	2,122	5	0	0

Table 11
The results of orderly charging scheduling for the entire week. DNLF represents the total load fluctuation within a week ($T = 672$), EVCC denotes the average charging cost of all EVs, and RECD indicates the average renewable energy consumption deficit per time slot.

Objective	DNLF	EVCC	RECD	SE	AST
Scenario0	695.11	25.89	192.47	–	–
Scenario1	664.67	24.98	–	0.092,7%	2.00
Scenario2	672.16	25.28	188.88	0.092,7%	2.25
Scenario3	647.83	23.83	–	0.088,3%	2.28
Scenario4	667.74	24.71	191.56	0.088,2%	2.37

(2) Scheduling results over a week

This section takes into account the charging behaviors of both fast- and slow-charging EVs on weekends and weekdays. Using the actual daily arrival numbers of EVs shown in Table 5 and integrating with the renewable energy generation forecast model, a week-long simulation was conducted for the Lucheng charging station. In the simulation, each EV was first assigned to a charging pile, and then a charging schedule was developed and implemented. Four orderly charging scheduling scenarios were considered:

Scenario 1: The optimization objective solely focuses on DNFL and EVCC, neglecting the constraints of renewable energy generation and V2G capability.

Scenario 2: All three objectives are considered, except for the V2G capability constraint.

Scenario 3: The optimization model only considers DNFL and EVCC, neglecting the renewable energy generation constraint.

Scenario 4: The optimization model takes into account both the objectives and constraints.

The basic load data of a residential community in Beijing were used as the predicted basic load of one week, as shown in Fig. 14(a). By incorporating real-time wind speed and light intensity data from San Francisco, the predicted power curves for wind turbines and photovoltaic power generation were derived. The charging scheduling results for a week are presented in Fig. 14. For clarity, the results for Tuesday are separately illustrated in Fig. 15, with different colors representing TOU. The changes in the total load combining the base and EV loads are depicted in Figs. 14(b) and Fig. 15(e). It can be observed that, compared to disorderly charging, the total load fluctuation is reduced in all the four scenarios, with the load shifting from the peak to the valley period. This load shifting is beneficial for the grid as it helps balance the power demand over time. The charging scheduling results in Fig. 14(c)–(f) indicate that the EV charging loads shift from the peak to the normal period in all the four scenarios. The total V2G discharging power during the valley period is significantly lower than that during the normal and peak periods. The RECD fluctuates around 0, suggesting that renewable energy is effectively utilized in real-time during the charging and discharging processes. As shown in Fig. 15(f), the deviations between the expected and actual end SOCs are within a reasonable range.

The charging scheduling results for the entire week are presented in Tables 10 and 11, with the daily simulation results provided in Appendix A-1. The abandonment rate, waiting time, and charging scheduling participation rate are 0.23%, 0%, and 97.70%, respectively, and the success rate of solving the optimization formulation is 100%. These verify the effectiveness of the proposed charging scheduling scheme and its ability to meet real-time implementation requirement.

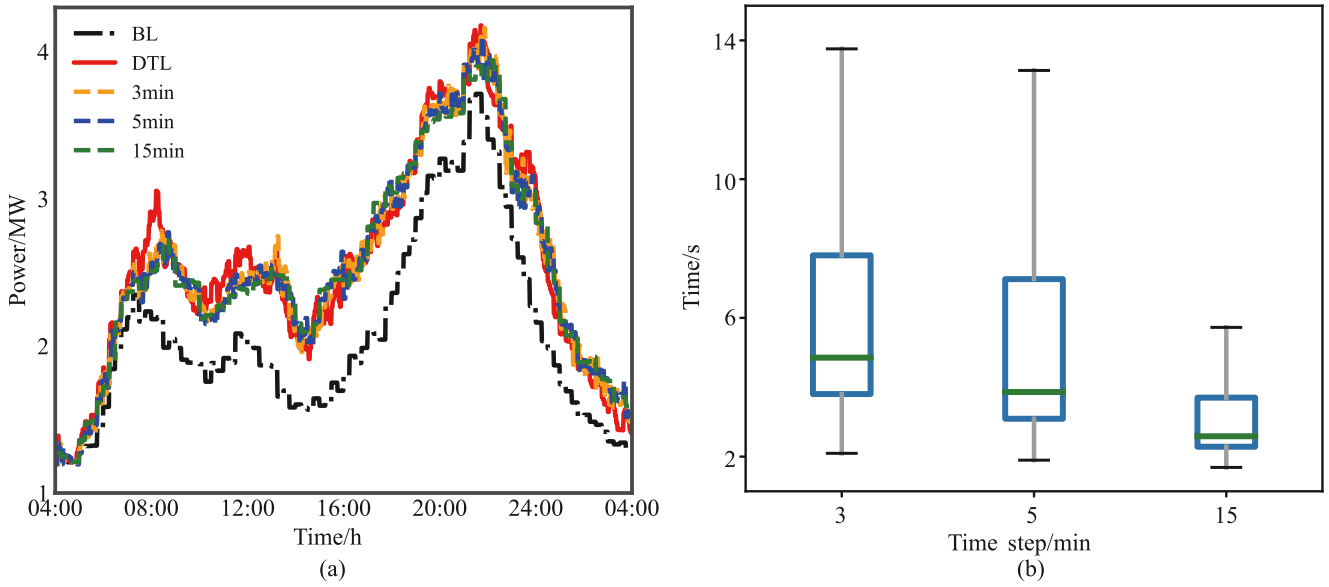

Fig. 16. Comparison at different time resolutions: (a) Orderly charging load. (b) Solution derivation time.

Furthermore, fluctuations in charging demand and variations in renewable energy generation emerge as two sensitivity factors that significantly influence the attainment of the study's objectives. Concerning charging demand fluctuations, as vividly illustrated in Figs. 3 and 15, the number of EVs arriving at the charging station varies across different periods throughout the day. Fewer EVs charge from 04:00–08:00 and 20:00–04:00, with lower overall load and reduced fluctuation at night compared to 08:00–20:00. Fig. 14 indicates that renewable energy generation on Tuesday is much higher than on Friday, with its consumption curve fluctuating around zero. This means EV charging mainly employ renewable energy. Appendix 1 shows higher renewable energy generation reduces the values of the three proposed indicators. It indicates that the proposed charging scheduling scheme can effectively balance the conflicting objectives. Moreover, it can efficiently integrate driving behaviors into the charging scheduling process, while also taking into account the concerns of grid operation, charging costs, and renewable energy integration.

(3) Impact of time step selection

The simulation encompasses 503 EVs, among which there are 350 fast-charging EVs and 153 slow-charging EVs. The vehicle-to-charging pile ratio is set to be the same as that in Section 5.2.1. The renewable energy generation and the basic load are presented in14(a), and it is designated as Scenario 4.

The duration of the time step for charging scheduling is adjustable. To determine the optimal time step, simulations were carried out with the durations of 3 min, 5 min, and 15 min. The results are presented in Fig. 16(a) and Table 12. It is evident that increasing the time-step duration has only little influence on the performance of the proposed scheme but can remarkably reduce the computational intensity. In practical applications, when the idle time of EVs is sufficiently long, a long time-step duration is recommended to shorten the optimization-solving time; when the EV idle time is restricted, a short time-step duration is advisable to better accomodate renewable energy generation.

Table 12
Comparison of different time steps. (DNLF represents the total load fluctuation within a day ($T = 96$), EVCC denotes the average charging cost of all EVs, and RECD indicates the average renewable energy consumption deficit per time slot.)

Time step/min	DNLF	EVCC	RECD	AST	FSN
3	694.56	11.77	377.01	6.84	6
5	686.06	11.81	374.08	5.09	0
15	676.73	11.53	370.87	2.96	0

6. Conclusion

This paper proposes a real-time charging scheduling scheme to enable efficient Vehicle-to-Grid interactions and facilitate renewable energy integration at public charging stations. A charging pile allocation mechanism is proposed, which can increase the utilization rate of charging piles, reduce EV waiting time, waiting rate, and abandonment rate, and determine the optimal vehicle-to-charging pile ratio. An orderly charging scheme based on a sliding window mechanism is also developed. Numerical results show that the proposed scheme can reduce the distribution network load fluctuation, average charging cost, and real-time energy consumption difference. Future research will further incorporate the impacts of traffic flow and distribution capacity limitations.

CRediT authorship contribution statement

Lei Zhang: Writing – original draft, Investigation, Funding acquisition, Formal analysis. **Yingjun Ji:** Writing – original draft, Investigation, Data curation. **Xiaohui Li:** Resources, Formal analysis. **Zhijia Huang:** Data curation, Conceptualization. **Dingsong Cui:** Writing – review & editing, Visualization. **Haibo Chen:** Resources, Project administration. **Jingyu Gong:** Writing – review & editing, Resources. **Fabian Breer:** Validation, Methodology. **Mark Junker:** Resources, Project administration. **Dirk Uwe Sauer:** Supervision, Funding acquisition.

Declaration of competing interest

The authors declare that they have no known competing financial interests or personal relationships that could have appeared to influence the work reported in this paper.

Lei Zhang reports financial support was provided by the Ministry of Science and Technology of the People's Republic of China.

Acknowledgements

This work was supported in part by the Ministry of Science and Technology of the People's Republic of China [Grant No. 2022YFE0103000]. This work was also jointly supported by several international projects, namely EU-funded projects ZEV - UP (No.101138721), ePowerMove (No.101192753), and FlexFleet (No.03EMF0407) funded by the German Federal Ministry for Digital and Transport and the EU.

A Appendix.

Table A-1
Specific numerical values of various indicators calculated for the entire week. (DNLF represents the total load fluctuation within a day ($T = 96$), EVCC denotes the average charging cost of all EVs, and RECD indicates the average renewable energy consumption deficit per time slot.)

Part	Day	Mon	Tue	Wed	Thu	Fri	Sat	Sun
Indicators	EVN	288	320	321	316	281	336	310
	POCN	277	310	313	310	278	331	303
	ACN	1	1	1	1	0	0	1
	WCN	0	0	0	0	0	0	0
Scenario0	DNLF	671.92	667.31	685.95	665.47	672.17	627.70	785.10
	EVCC	26.12	25.62	25.32	25.39	26.79	26.33	25.73
	RECD	182.89	103.55	188.80	165.49	224.10	199.95	176.43
Scenario1	DNLF	651.73	628.90	674.09	628.81	644.00	636.58	758.03
	EVCC	25.07	24.95	24.26	24.68	25.82	25.14	25.04
Scenario2	DNLF	657.81	632.09	685.25	636.11	655.07	642.39	765.70
	EVCC	25.33	25.06	24.58	24.94	26.37	25.50	25.30
	RECD	168.12	117.52	212.64	165.27	229.82	240.47	188.30
Scenario3	DNLF	632.70	614.12	657.96	608.90	625.44	616.12	746.40
	EVCC	23.74	23.97	23.18	23.45	24.40	24.08	24.04
Scenario4	DNLF	647.53	627.72	680.80	628.05	650.77	639.60	767.55
	EVCC	24.59	24.32	24.03	24.48	25.69	24.99	24.96
	RECD	170.44	120.16	216.46	176.13	230.20	240.29	187.26

Table A-2
Partial entries of the preprocessed electric vehicle charging behavior database.

Start time	End time	Start SOC/%	End SOC/%	Battery/kWh	Fast/Slow charging	Workday/Holiday
2021-01-09 21:09:56	2021-01-10 02:07:45	15	98	52	Fast charging	Holiday
2021-01-10 02:07:46	2021-01-10 20:08:31	8	100	65	Slow charging	Holiday
2021-01-20 08:04:31	2021-01-20 10:03:22	11	100	52	Fast charging	Workday
2021-01-21 09:09:06	2021-01-21 21:46:21	5	98	48	Slow charging	Workday

References

[1] Ermias Benti Natei, Diro Chaka Mesfin, Gezahegn Semie Addisu. Forecasting renewable energy generation with machine learning and deep learning: current advances and future prospects. Sustainability 2023;15(9):7087.
[2] Tansel Tugcu Can, Menegaki Angeliki N. The impact of renewable energy generation on energy security: evidence from the g7 countries. Gondwana Res 2024;125:253–65.
[3] He Hongwen, Sun Fengchun, Wang Zhenpo, Lin Cheng, Zhang Chengning, Xiong Rui, et al. China's battery electric vehicles lead the world: achievements in technology system architecture and technological breakthroughs. Green Energy and Intelligent Transportation 2022;1(1):100020.
[4] Blaabjerg Frede, Yang Yongheng, Kim Katherine A, Rodriguez Jose. Power electronics technology for large-scale renewable energy generation. Proc IEEE 2023;111(4):335–55.
[5] Kataray Tarun, Nitesh B, Yarram Bharath, Sinha Sanyukta, Cuce Erdem, Shaik Saboor, et al. Integration of smart grid with renewable energy sources: opportunities and challenges–a comprehensive review. Sustain Energy Technol Assessments 2023;58:103363.
[6] Xu Penghui, Wang Xiaobo, Li Zhichao. Impact and optimization of vehicle charging scheduling on regional clean energy power supply network management. Energy Informatics 2025;8(1):13.
[7] Loni Abdolah, Asadi Somayeh. Data-driven equitable placement for electric vehicle charging stations: case study san francisco. Energy 2023;282:128796.
[8] Roy Pranoy, Ilka Reza, He Jiangbiao, Liao Yuan, Cramer Aaron M, Mccann Justin, et al. Impact of electric vehicle charging on power distribution systems: a case study of the grid in western Kentucky. IEEE Access 2023;11:49002–23.
[9] Manz Devon, Walling Reigh, Miller Nick, LaRose Beth, D'Aquila Rob, Daryanian Bahman. The grid of the future: ten trends that will shape the grid over the next decade. IEEE Power Energy Mag 2014;12(3):26–36.
[10] Gong Jingyu, Wasylowski David, Figgener Jan, Bihn Stephan, Rücker Fabian, Ringbeck Florian, et al. Quantifying the impact of v2x operation on electric vehicle battery degradation: an experimental evaluation. ETransportation 2024;20:100316.
[11] Ahmed Elsanabary, Khairullah Karam, Aziz Nur Fadilah Ab, Mekhilef Saad. Power management and optimized control of hybrid pv-bess-grid integrated fast ev charging stations. J Energy Storage 2024;90:111802.
[12] Srivastava Abhishek, Saravanan S. Harmonic mitigation using optimal active power filter for the improvement of power quality for a electric vehicle changing station. e-Prime-Advances in Electrical Engineering, Electronics and Energy 2024;8:100527.
[13] Li Mince, Wang Yujie, Peng Pei, Chen Zonghai. Toward efficient smart management: a review of modeling and optimization approaches in electric vehicle-transportation network-grid integration. Green Energy and Intelligent Transportation 2024:100181.
[14] Dik Abdullah, Omer Siddig, Boukhanouf Rabah. Electric vehicles: V2g for rapid, safe, and green ev penetration. Energies 2022;15(3):803.
[15] Huang Yongyi, Masrur Hasan, Lipu Molla Shahadat Hossain, Or Rashid Howlader Harun, Gamil Mahmoud M, Nakadomari Akito, et al. Multi-objective optimization of campus microgrid system considering electric vehicle charging load integrated to power grid. Sustain Cities Soc 2023;98:104778.
[16] Yao Zhaosheng, Wang Zhiyuan, Ran Lun. Smart charging and discharging of electric vehicles based on multi-objective robust optimization in smart cities. Appl Energy 2023;343:121185.
[17] Li Xiaohui, Wang Zhenpo, Zhang Lei, Sun Fengchun, Cui Dingsong, Hecht Christopher, et al. Electric vehicle behavior modeling and applications in vehicle-grid integration: an overview. Energy 2023;268:126647.
[18] Zheng Jinghong, Wang Xiaoyu, Men Kun, Zhu Chun, Zhu Shouzhen. Aggregation model-based optimization for electric vehicle charging strategy. IEEE Trans Smart Grid 2013;4(2):1058–66.
[19] Jan Figgener, Tepe Benedikt, Rücker Fabian, Schoeneberger Ilka, Hecht Christopher, Jossen Andreas, et al. The influence of frequency containment

reserve flexibilization on the economics of electric vehicle fleet operation. J Energy Storage 2022;53:105138.
[20] Wu Shengcheng, Pang Aiping. Optimal scheduling strategy for orderly charging and discharging of electric vehicles based on spatio-temporal characteristics. J Clean Prod 2023;392:136318.
[21] Fiori Chiara, Ahn Kyoungho, Rakha Hesham A. Power-based electric vehicle energy consumption model: model development and validation. Appl Energy 2016;168:257–68.
[22] Quirós-Tortós Jairo, Ochoa Luis F, Lees Becky. A statistical analysis of ev charging behavior in the UK. In: 2015 IEEE PES innovative smart grid technologies Latin America (ISGT LATAM). IEEE; 2015. p. 445–9.
[23] Cui Dingsong, Wang Zhenpo, Liu Peng, Zhang Zhaosheng, Wang Shuo, Zhao Yiwen, et al. Coordinated charging scheme for electric vehicle fast-charging station with demand-based priority. IEEE Trans Transport Electrif 2024;10:6449–59.
[24] Li Zhi, Chen Zhibin, Li Hailong, Guan ChengHe, Zhong Minghui. On the value of orderly electric vehicle charging in carbon emission reduction. Transport Res Transport Environ 2024;135:104383.
[25] Chen Qin, Folly Komla Agbenyo. Application of artificial intelligence for ev charging and discharging scheduling and dynamic pricing: a review. Energies 2022;16(1):146.
[26] Makeen Peter, Memon Saim, Elkasrawy MA, Abdullatif Sameh O, Ghali Hani A. Smart green charging scheme of centralized electric vehicle stations. Int J Green Energy 2022;19(5):490–8.
[27] Hwang Goh Hui, Zong Lian, Zhang Dongdong, Dai Wei, Lim Chee Shen, Kurniawan Tonni Agustiono, et al. Orderly charging strategy based on optimal time of use price demand response of electric vehicles in distribution network. Energies 2022;15(5):1869.
[28] Yue Yuntao, Zhang Qihui, Zhang Jiaran, Liu Yufan. Orderly charging and discharging group scheduling strategy for electric vehicles. Appl Sci 2023;13(24):13156.
[29] Ali Saadon Al-Ogaili, Hashim Tengku Juhana Tengku, Rahmat Nur Azzammudin, Ramasamy Agileswari K, Marsadek Marayati Binti, Faisal Mohammad, et al. Review on scheduling, clustering, and forecasting strategies for controlling electric vehicle charging: challenges and recommendations. IEEE Access 2019;7:128353–71.
[30] Li Xiaohui, Wang Zhenpo, Zhang Lei, Huang Zhijia, Cui Dingsong, Li Weihan, et al. A comparative study of real-time coordinate charging schemes for residential electric vehicles. J Energy Storage 2024;98:113021.
[31] Wang Yujie, Kang Xu, Chen Zonghai. A survey of digital twin techniques in smart manufacturing and management of energy applications. Green Energy and Intelligent Transportation 2022;1(2):100014.
[32] Zhang Zhaoyun, Lv Linjun. Status and development of research on orderly charging and discharging of electric vehicles. Electronics 2023;12(9):2041.
[33] Qi Kang, Feng ShuWei, Zhou MengChu, Ahmed Chiheb Ammari, Sedraoui Khaled. Optimal load scheduling of plug-in hybrid electric vehicles via weight-aggregation multi-objective evolutionary algorithms. IEEE Trans Intell Transport Syst 2017;18(9):2557–68.
[34] Du Wenyi, Ma Juan, Yin Wanjun. Orderly charging strategy of electric vehicle based on improved pso algorithm. Energy 2023;271:127088.
[35] Zhang Meijuan, Yan Qingyou, Guan Yajuan, Ni Da, Tinajero Gibran David Agundis. Joint planning of residential electric vehicle charging station integrated with photovoltaic and energy storage considering demand response and uncertainties. Energy 2024;298:131370.
[36] Yin Wanjun, Jia Leilei, Ji Jianbo. Energy optimal scheduling strategy considering v2g characteristics of electric vehicle. Energy 2024;294:130967.
[37] Ding Yan, Zhu Yan, Wang Qiaochu, Tian Zhe, Yan Rui, Yan Zhe, et al. A comprehensive scheduling model for electric vehicles in office buildings considering the uncertainty of charging load. Int J Electr Power Energy Syst 2023;151:109154.
[38] Pourvaziri H, Sarhadi H, Azad N, Afshari H, Taghavi M. Planning of electric vehicle charging stations: an integrated deep learning and queueing theory approach. Transport Res E Logist Transport Rev 2024;186:103568.
[39] Zhu Jie, Li Yixin, Yang Jun, Li Xianglong, Zeng Shuang, Chen Yanxie. Planning of electric vehicle charging station based on queuing theory. J Eng 2017;(13):1867–71. 2017.
[40] Zaidi Imene, Oulamara Ammar, Idoumghar Lhassane, Basset Michel. Electric vehicle charging scheduling problem: heuristics and metaheuristic approaches. SN Computer Science 2023;4(3):283.
[41] Zhang Guoyu, Dai Mian, Zhao Shuai, Zhu Xianglei. Orderly automatic real-time charging scheduling scenario strategy for electric vehicles considering renewable energy consumption. Energy Rep 2023;9:72–84.
[42] Yang Ao, Wang Honglei, Li Bin, Tan Zhukui. Capacity optimization of hybrid energy storage system for microgrid based on electric vehicles' orderly charging/discharging strategy. J Clean Prod 2023;411:137346.
[43] Pan Kui, Liang Chuan-Dong, Lu Min. Optimal scheduling of electric vehicle ordered charging and discharging based on improved gravitational search and particle swarm optimization algorithm. Int J Electr Power Energy Syst 2024;157:109766.
[44] Ren Lina, Yuan Mingming, Jiao Xiaohong. Electric vehicle charging and discharging scheduling strategy based on dynamic electricity price. Eng Appl Artif Intell 2023;123:106320.
[45] Yin WanJun, Wen Tao, Zhang Chao. Cooperative optimal scheduling strategy of electric vehicles based on dynamic electricity price mechanism. Energy 2023;263:125627.
[46] Zhang Zhaoyun, Wang Xinghua. Research on dynamic time-sharing tariff orderly charging strategy based on nsga2 in pv-storage-charging stations. Elec Power Syst Res 2023;225:109784.
[47] Chen Jiajie, Hou Hui, Wu Wenjie, Wu Xixiu. Optimal operation between electric power aggregator and electric vehicle based on stackelberg game model. Energy Rep 2023;9:699–706.
[48] Yusoff Yusliza, Ngadiman Mohd Salihin, Zain Azlan Mohd. Overview of nsga-ii for optimizing machining process parameters. Procedia Eng 2011;15:3978–83.
[49] Çelikbilek Yakup, Tüysüz Fatih. An in-depth review of theory of the topsis method: an experimental analysis. Journal of Management Analytics 2020;7(2):281–300.
[50] McLachlan Geoffrey J, Rathnayake Suren. On the number of components in a Gaussian mixture model. Wiley Interdisciplinary Reviews: Data Min Knowl Discov 2014;4(5):341–55.
[51] Cui Dingsong, Wang Zhenpo, Liu Peng, Wang Shuo, Zhang Zhaosheng, Dorrell David G, et al. Battery electric vehicle usage pattern analysis driven by massive real-world data. Energy 2022;250:123837.
[52] Usman Tahir Muhammad, Sangwongwanich Ariya, Stroe Daniel-Ioan, Blaabjerg Frede. Multi-objective optimization for multi-stage constant current charging for li-ion batteries. J Energy Storage 2024;86:111313.
[53] Jiang Linru, Diao Xiaohong, Zhang Yuanxing, Zhang Jing, Li Taoyong. Review of the charging safety and charging safety protection of electric vehicles. World Electric Vehicle Journal 2021;12(4):184.
[54] Dong Haoxuan, Wang Qun, Zhuang Weichao, Yin Guodong, Gao Kun, Li Zhaojian, et al. Flexible eco-cruising strategy for connected and automated vehicles with efficient driving lane planning and speed optimization. IEEE Trans Transport Electrif 2024;10:1530–40.
[55] Deb Naireeta, Singh Rajendra, Brooks Richard R, Bai Kevin. A review of extremely fast charging stations for electric vehicles. Energies 2021;14(22):7566.
[56] Bhardwaj Pooja, Bali Vikram, Kaur Jaspreet. A review on load balancing and site selection of electric vehicle charging station. Transport 2020;1(2):3–4.
[57] Dong Haoxuan, Hu Qiuhao, Li Dongjun, Li Zhaojian, Song Ziyou. Predictive battery thermal and energy management for connected and automated electric vehicles. IEEE Trans Intell Transport Syst 2025;26:2144–56.